

REVIEW

Open Access



Revolutionizing lymph node metastasis imaging: the role of drug delivery systems and future perspectives

Ze-Min Cai^{1†}, Zi-Zhan Li^{1†}, Nian-Nian Zhong^{1†}, Lei-Ming Cao¹, Yao Xiao¹, Jia-Qi Li¹, Fang-Yi Huo¹, Bing Liu^{1,2}, Chun Xu⁴, Yi Zhao^{1,3}, Lang Rao^{5*} and Lin-Lin Bu^{1,2*}

Abstract

The deployment of imaging examinations has evolved into a robust approach for the diagnosis of lymph node metastasis (LNM). The advancement of technology, coupled with the introduction of innovative imaging drugs, has led to the incorporation of an increasingly diverse array of imaging techniques into clinical practice. Nonetheless, conventional methods of administering imaging agents persist in presenting certain drawbacks and side effects. The employment of controlled drug delivery systems (DDSs) as a conduit for transporting imaging agents offers a promising solution to ameliorate these limitations intrinsic to metastatic lymph node (LN) imaging, thereby augmenting diagnostic precision. Within the scope of this review, we elucidate the historical context of LN imaging and encapsulate the frequently employed DDSs in conjunction with a variety of imaging techniques, specifically for metastatic LN imaging. Moreover, we engage in a discourse on the conceptualization and practical application of fusing diagnosis and treatment by employing DDSs. Finally, we venture into prospective applications of DDSs in the realm of LNM imaging and share our perspective on the potential trajectory of DDS development.

Highlights

1. The shortcomings inherent in traditional methods of administering imaging agents and the application of drug delivery systems (DDSs) across diverse imaging techniques are elucidated.
2. The pivotal role that DDSs play in specifically targeting metastatic lymph node (LN) imaging and integrating the diagnosis and treatment of lymph node metastasis (LNM) is discussed.
3. The potential risks associated with the targeting of LNs using DDSs are detailed.
4. The prospects of utilizing DDSs in LNM imaging are explored, and insights are provided regarding the anticipated trajectory of DDSs' future development.

[†]Ze-Min Cai, Zi-Zhan Li and Nian-Nian Zhong have contributed equally to this work.

*Correspondence:

Lang Rao

lr Rao@szbl.ac.cn

Lin-Lin Bu

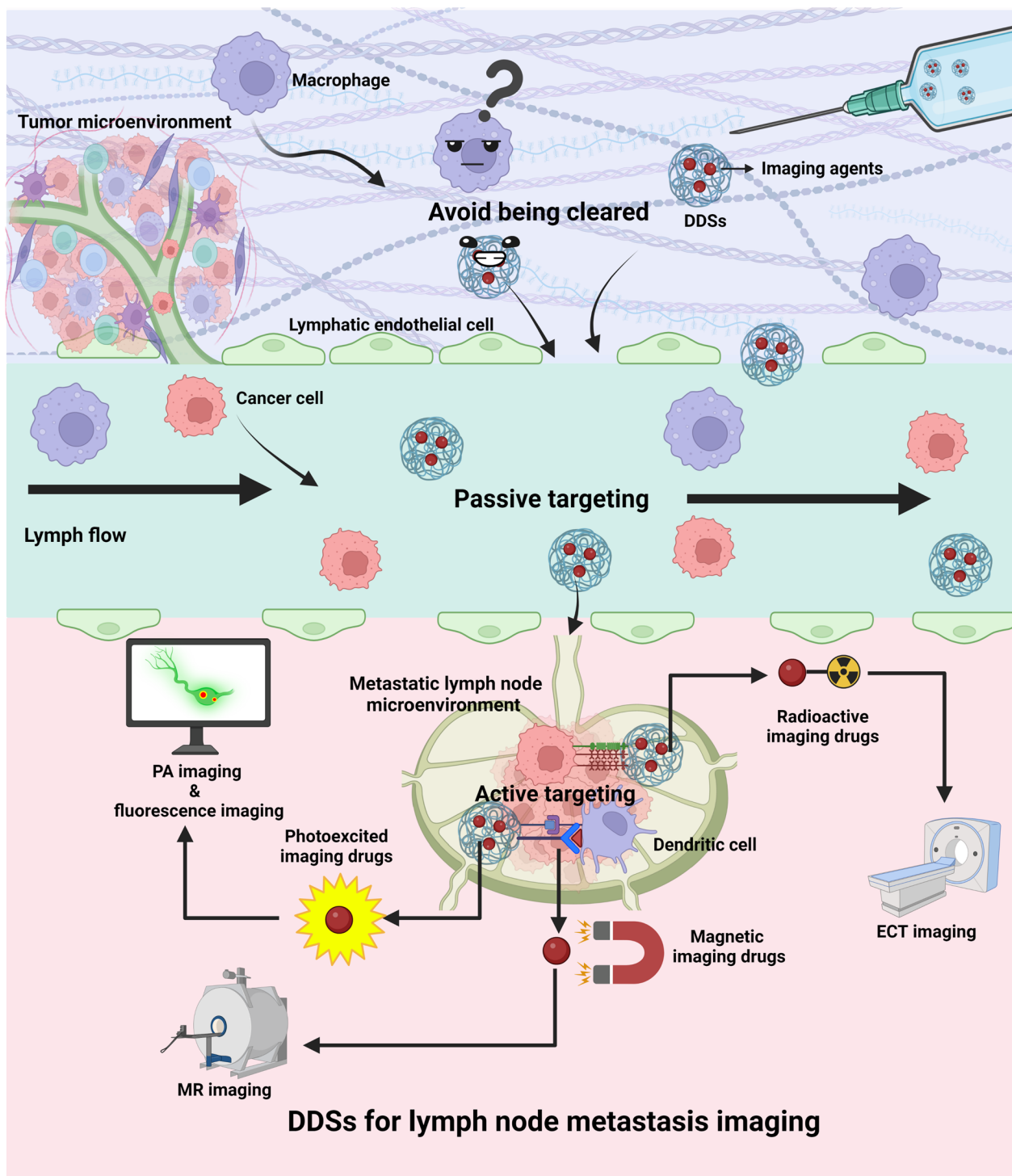
lin-lin.bu@whu.edu.cn

Full list of author information is available at the end of the article



Keywords Drug delivery systems, Lymph node metastasis, Imaging, Computed tomography, Magnetic resonance

Graphical Abstract



Introduction

Cancer stands as a paramount global public health concern, assuming the second rank after cardiovascular disease in terms of mortality [1]. Lymphatic invasion and subsequent metastasis to lymph nodes (LNs), leading to the propagation to other regions of the body, is a predominant characteristic of cancer cells [2]. Lymph node metastasis (LNM) significantly contributes to cancer-related mortalities and forms a key determinant in assessing the survival and prognosis of patients [3, 4]. The societal and healthcare burden attributable to cancer’s lymphatic metastasis is substantial, posing a serious threat to human health and survival.

LNs, as secondary lymphatic organs, have crucial roles in facilitating immune evasion by cancer cells and serve as primary routes for metastatic dissemination, especially in cancers such as breast, and head and neck cancer [5, 6]. LNM is indicative of a grim prognosis and functions as a relay station and booster for distant metastasis, thereby profoundly influencing survival time and life quality of patients. Moreover, LNM significantly impacts the TNM staging, guiding the treatment decision-making process which frequently involves surgical intervention for lymphatic metastasis [7].

Up to now, LN dissection remains one of the main methods for treating LNM. Although current diagnostic techniques are multifarious, imaging examination still serves as the mainstay for diagnosing LNM. The development of LN dissection evolves with the renewal of treatment concepts and the advancement of basic theories. The determination of the surgical range often depends on the imaging diagnosis; thus, defective diagnostic performance may result in a poor prognosis, such as occult LNM [8]. Furthermore, the implementation of excessive surgical procedures may also result in many adverse outcomes, such as nerve damage, pneumothorax, chyle leak, lymphedema, etc., which further lead to physiological dysfunction, disability, appearance damage, and even death [9–14]. Therefore, improving diagnostic efficiency and accurately identifying tumor LNM is critical for early cancer diagnosis and treatment, precise staging, and prognosis prediction, ultimately contributing to the reduction of missed diagnoses and treatment side effects. This improvement helps in identifying the presence of LNM, distant metastasis, and other complications. ultimately aiming to improve patient survival and quality of life [15].

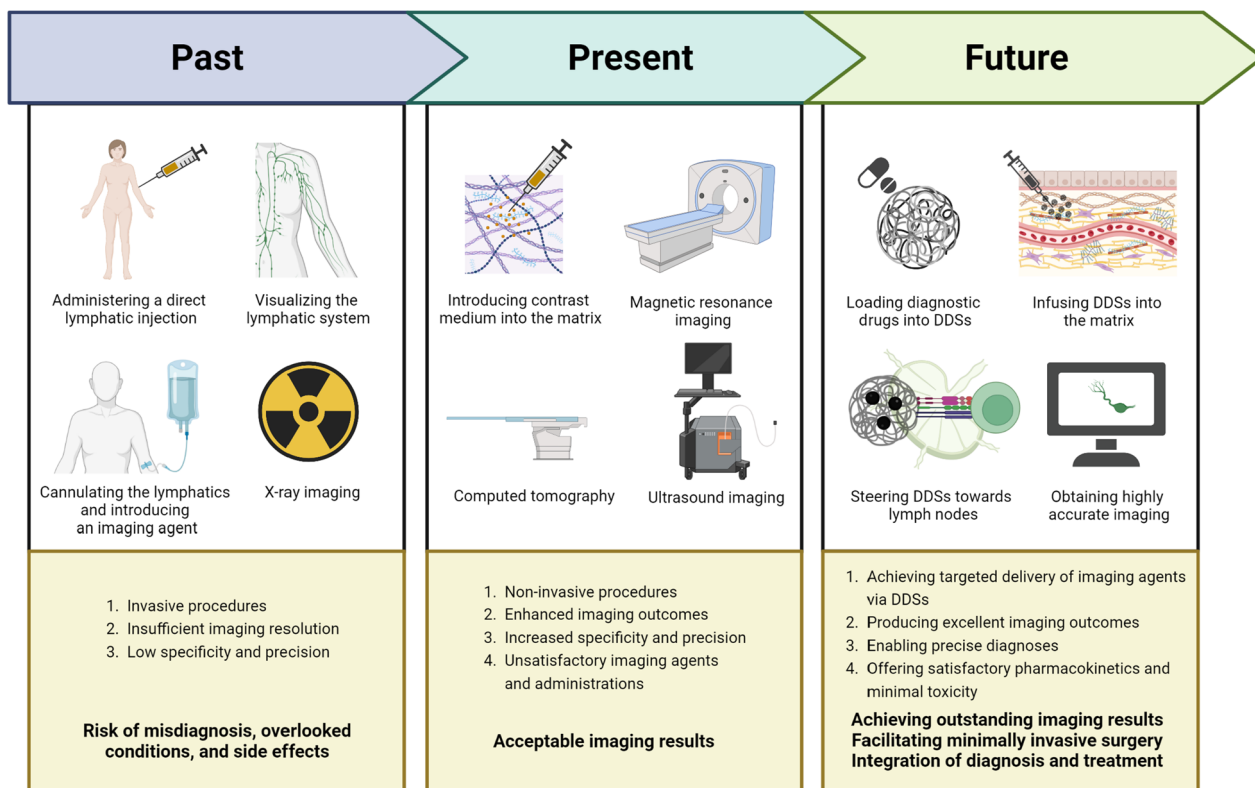


Fig. 1 The chronological progression—past, present, and anticipated future—of lymph node (LN) imaging via the medium of drug delivery systems (DDSs). Created with BioRender.com

Medical imaging has been instrumental in diagnosing LNM. In the past, clinicians typically used X-rays to diagnose LNM. Currently, commonly used imaging techniques in the diagnosis of LNM include computed tomography (CT), magnetic resonance imaging (MRI), and ultrasound (US) imaging, among others (Fig. 1). Because the density difference between LNs and surrounding tissues is low, the introduction of contrast agents can effectively improve LNs contrast, making the image easier to identify and increasing the diagnostic performance. Contrast agents significantly enhance the visual differentiation of lymphoid tissue, bolstering diagnostic capabilities. The combination of various imaging techniques and contrast agents can achieve accurate and minimally invasive visualization of LNM [16]. However, traditional contrast agent administration faces issues such as lack of targeting, brief fluid retention time, a single imaging modality, and limited detection points; some contrast agents may also produce renal and nerve toxicity [17, 18]. It has been reported that reversible acute renal failure may occur shortly after the injection of a radioactive contrast agent, possibly due to the direct induction of renal tubular epithelial cell toxicity and renal medulla ischemia [17]. Moreover, the use of gadolinium-based contrast agents is closely related to renal systemic fibrosis and gadolinium accumulation in the brain [19]. This evidence has the potential to influence the use of contrast agents in LNM imaging. Given the limitations of traditional administration methods and the importance of accurate imaging in the diagnosis of LNM, it is urgent to propose new methods of imaging agent delivery.

Controlled drug delivery systems (DDSs) are specialized devices designed to precisely deliver drugs to targeted sites within the body. Composed of the drug (imaging agent), a targeting component, and a carrier, they form an interactive system capable of specifically delivering diagnostic agents to biological targets. Through modification, contrast agents can effectively avoid clearance by phagocytes and actively target specific sites in LNs. Some studies have shown that DDSs are highly retained in metastatic LNs due to the enhanced permeability and retention (EPR) effect. Leveraging both active and passive targeting effects, these systems offer optimized delivery of imaging agents for superior diagnostic efficacy and biosafety, facilitated by accurate drug release sites, rates, and times, compared to traditional administration methods. Some DDSs also allow fluorescence imaging techniques to image longer wavelengths beyond the traditional near-infrared (NIR) region, effectively reducing molecular scattering and interference from endogenous substances [20]. Additionally, DDSs are ideal for combining two or more

contrast agents to overcome the limitations of a single imaging modality. These characteristics enable DDSs to provide accurate diagnosis and guidance for subsequent treatment.

DDSs have emerged as promising new vehicles for the delivery of imaging agents, with researchers emphasizing the pivotal role of the carrier in the DDSs' targeting ability. Present research primarily focuses on nanomaterial carriers such as nanoparticles (NPs), and microbubbles [21, 22], that endow controlled DDSs with unique adjustability, surface effects, and size effects [23, 24]. Given the essential role of LNM localization in directing cancer staging and treatment outcomes, the amalgamation of DDSs with CT, MRI, and other imaging techniques for LNM imaging has drawn considerable attention [25–27]. DDSs exhibit properties that enable rapid clearance from the injection site, targeted transport facilitated by the targeting component [28], and evasion of the reticular endothelial system (RES) phagocytosis effect, leading to retention in LN [29, 30]. This enhances LN imaging accuracy, ensures precise metastasis localization, and reduces non-target accumulation and the dosage and toxicity of diagnostic drugs. The use of DDSs effectively mitigates the need for LN dissection, lowers postoperative recurrence rates and side effects [31], establishing DDSs as a promising avenue for metastatic LN imaging research.

In this review, we present an overview of the evolution of LN imaging, and outline the application of commonly used DDSs in conjunction with various imaging techniques for LNM imaging (Fig. 1). Furthermore, we delve into the concept and implementation of integrated diagnosis and treatment using DDSs. Lastly, we discuss the potential of DDSs in LN imaging and present our insights into the future developmental trajectory of DDSs.

Brief history

The genesis of medical imaging can be traced back to 1895 when Röntgen captured the world's first X-ray image of a human hand [32]. This pioneering effort marked the birth of medical imaging and catalyzed its continuous evolution, significantly contributing to disease diagnosis and treatment. In 1915, Dewis and colleagues advocated for the use of imaging tests to aid in the diagnosis of LNM when conventional diagnostic means fell short, thus averting unnecessary exploratory surgeries [33]. This initiated a novel paradigm for diagnosing subsequent LNM. By 1938, Warren et al., through their analysis of soft tissue sarcoma hospitalization cases, discovered that 5–10% of sarcomas had LNM, emphasizing the critical role of LNs in human tumor metastasis [34].

In 1971, the introduction of CT to clinical practice marked another milestone, further bolstered by Ambrose et al.'s application of CT in clinical trials [35]. This development advanced digital radiographic technology and enriched the diagnostic capabilities for ensuing diseases [36]. By 1977, Mancuso and colleagues utilized CT to appraise the association between primary lesions of laryngeal cancer and LNM, providing a foundation for subsequent CT applications in LNM diagnosis [37]. A year later, Carter successfully employed lymphoscintigraphy (LSG) to analyze LNM in breast cancer patients, obtaining satisfactory imaging results [38]. This feasibility study helped establish LSG as the gold standard for clinical lymph imaging [39].

In 1992, Husband et al. integrated MRI into the imaging of LNM in bladder cancer, yielding enhanced contrast between LNs and blood vessels as compared to prior imaging techniques [40]. In 2004, indocyanine green (ICG), the first cyanine dye approved by the US Food and Drug Administration (FDA), was utilized for sentinel lymph node (SLN) detection in gastric cancer patients in combination with the NIR lymphography technique [41], affirming the utility of NIR lymphography in diagnosing LNM.

The evolution of DDSs was catalyzed in 1952 by the development of the first controlled release preparation by Smith and colleagues [42]. Subsequently, in 1976, Kreuter introduced the concept of “nanoparticle” in medicine [43]. As effective carriers and imaging drugs, NPs have progressively found their place in DDSs. In 1984, Nefzger

and colleagues discovered that NPs exhibited high retention in tissues such as LNs, liver, stomach, and bone marrow post-administration, foreshadowing the successful application of DDSs in LNM imaging [44].

In 1989, Pouliquen and colleagues engineered a superparamagnetic NP to function as a contrast agent for liver MRI, effectively amplifying hepatic contrast and thus promoting the application of DDSs in imaging [45]. In 1994, Anzai et al. pioneered the application of DDSs in imaging LNM in head and neck cancer patients, observing that benign LNs exhibited significantly lower signal intensity than metastatic LNs post-injection, aiding in their differentiation and accurate diagnosis [46]. In 2004, Kobayashi and colleagues employed DDSs for lymph imaging by MRI to visualize the drainage from mouse mammary tumors to lymphatic vessels and LNs. The lymphatic drainage visualization capability of DDSs outperformed that of conventional administration methods, providing a clearer depiction of lymphatic drainage [47].

In 2009, Song and colleagues employed gold nanoclusters-based DDSs as imaging agents for NIR lymphography to map SLNs [48]. Subsequently, in 2011, Boll and colleagues injected NP-based DDSs into mice and found that DDSs provided strong contrast for abdominal, mediastinal LNs, and adrenal glands with a low dose requirement when monitoring liver diseases using micro-CT [49]. These advances highlight the potential of DDSs in precise imaging and differential diagnosis of tumor LNM, warranting further research and clinical applications (Fig. 2).

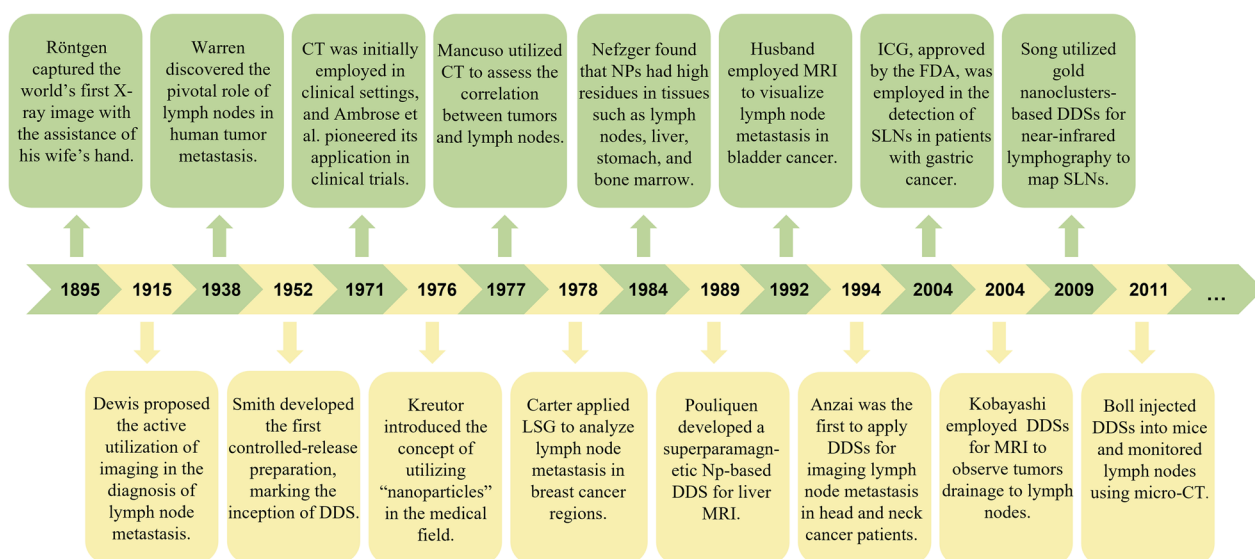


Fig. 2 A brief historical overview of lymph node metastasis imaging based on DDSs. DDS drug delivery system, CT computed tomography, LSG lymphoscintigraphy, NP nanoparticle, MRI magnetic resonance imaging, ICG indocyanine green, SLN sentinel lymph node

Cancer-induced alterations in LNs

The lymphatic system, which includes a multitude of organs such as the bone marrow, spleen, tonsils, thymus, and LNs, interconnected by lymphatic vessels, serves as the body's second vascular system. It plays crucial roles in maintaining fluid homeostasis and regulating adaptive immune responses [50]. The ensuing discussion explores LN modifications induced by cancer cell infiltration.

Imaging-based detection of metastatic alterations in LNs

Tumor metastasis to LNs causes changes in the size, shape, and structure of LNs, which can be detected by imaging examination to confirm the occurrence of LNM [51]. These modifications include cancer cell infiltration into LNs, eliciting inflammatory responses and altering the nodes' size and shape.

Apart from external morphological shifts, metastatic LNs may also undergo structural modifications. The edges of metastatic LNs are usually sharper than those of benign LNs, a characteristic related to tumor cell infiltration in LNs [52]. This is because the infiltration of normal LN tissue by cancer cells can enhance the acoustic impedance within the LN, making the boundaries more distinctive in imaging compared to normal LNs. Invasion by cancer cells can also compromise or obliterate the

fatty tissue in the hilum of the LN, leading to the loss of a low-density structure on imaging [53, 54]. However, a blurry border of a confirmed metastatic LN may indicate extracapsular infiltration by cancer cells, which usually indicates a worse prognostic outcome [55]. Additionally, metastatic LNs may exhibit features such as centrifugal cortical hypertrophy [56], intranodal necrosis [57], calcification, and the corresponding characteristics of the intranodal echogenic hilus, cystic area, or a punctate acoustic shadow, among other imaging features [58]. By identifying these alterations, imaging techniques can assist in diagnosing LNM.

In the past, there was no clear consensus on the diagnostic criteria for imaging LNM. The diagnosis of LN imaging still relied mainly on the experience of physicians. The introduction of the Node Reporting and Data System (Node-RADS) addressed this problem and facilitated the standardization of imaging evaluation of affected LNs [59]. Evaluation according to the size, configuration, boundary, and other categories within this system can effectively assess the involvement of LNs, providing a structured and repeatable criterion for the diagnosis of LNM to address the consensus and experience gap between radiologists. At the same time, it also reduces the risk of missed diagnosis due to

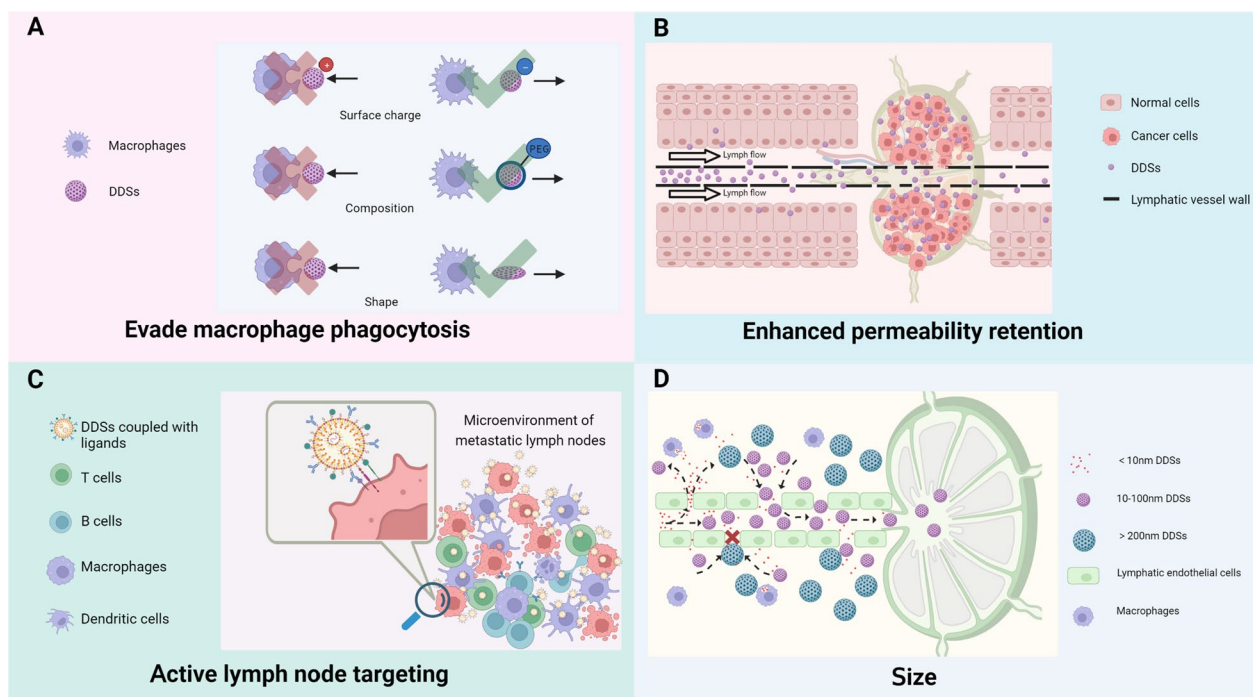


Fig. 3 The targeted lymph node mechanisms of drug delivery systems (DDSs). **A** By modifying their surface charge, composition, and shape, DDSs possess the capability to elude phagocytosis activity by macrophages. **B** Benefitting from the EPR effect, DDSs can maintain a persistent presence within metastatic lymph nodes. **C** Leveraging the use of ligand-coupled NPs, DDSs have the potential to actively home in on targeted lymph nodes. **D** DDSs, when tailored to a specific size, gain the ability to infiltrate lymphatic vessels in substantial volumes. Created with BioRender.com

varying diagnostic criteria (such as the missed diagnosis of micro-metastatic LNs) [60]. Currently, this system has been applied to the LN imaging of patients with bladder cancer, colon cancer, cholangiocarcinoma, lung cancer, etc. Compared with traditional non-standardized diagnostic criteria, the overall diagnostic performance of the new system has improved [60–63]. Nevertheless, these shape and structure changes should not be used as standalone diagnostic markers, and a definitive diagnosis requires a combination of multiple indicators and pathological examination results.

Physiological basis of DDS in LN imaging

Lymphatic capillaries, positioned at the terminus of the lymphatic system, gather lymphatic fluid from interstitial tissues and transport it back to the cardiovascular system via lymphatic vessels, thereby maintaining the fluid balance of the circulatory system. The broad intercellular space and high permeability of the endothelial cells in lymphatic capillaries facilitate the passage of interstitial fluid, which is subsequently collected as lymphatic fluid [16]. Capitalizing on this characteristic, DDSs with a diameter less than 200 nm can enter the lymphatic vessels and flow into the LNs [64].

During lymphatic return, macrophages remove foreign material. To evade macrophage clearance and amplify their passive targeting ability towards LNs, DDSs undergo specific modifications in shape, surface charge, and composition, effectively impeding their clearance by macrophages. In terms of shape modification, non-spherical NPs can effectively reduce the likelihood of clearance by phagocytes, whereas spherical NPs are more susceptible to blood convection and tend to drift laterally along the walls of blood or lymphatic vessels, thus reducing the likelihood of margination [65, 66]. Regarding surface charge, negatively charged DDSs enhance the efficiency of transport to LNs and effectively promote the activation of immune cells in the tumor microenvironment of metastatic LNs. They can be preferentially taken up by cancerous tissues and reduce the non-specific clearance of macrophages [67]. Concerning composition, the composition of DDSs affects the pharmacokinetics of their internal drugs and the immune system's clearance efficiency. For example, PEGylation—a technique that modifies compounds or supports by adding polymeric chains of ethylene glycol (or polyethylene oxide, or polyoxyethylene)—is a widely used DDS structure modification strategy. It endows DDSs with inertness and stability, mitigates the interaction between the drugs and the biological milieu, confers stealth effects on DDSs, diminishes protein adsorption, and prevents cellular ingestion

(Fig. 3A) [68–71]. It has been demonstrated that, compared to healthy LNs, metastatic LNs exhibit increased lymphatic vessel permeability and obstructed lymphatic drainage, which facilitate the retention of DDSs and augment their passive targeting effect through the EPR effect (Fig. 3B) [72].

LNs are known to house a profusion of immune cells such as dendritic cells (DCs), T cells, B cells, among others. These cells sample the incoming lymphatic fluid to capture antigens and initiate adaptive immune responses [73]. Upon entry into LNs, appropriately sized DDSs can be engulfed by antigen-presenting cells (APCs), thereby serving a passive targeting role (Fig. 3D). Furthermore, APCs in LNs express mannose receptors [74], CD11c [75], CD169, and other specific targets [76]. The cancer cell infiltration in metastatic LNs also exhibits abnormally high expression of molecules like CD44 [77]. Conjugation of DDSs to ligands for these targets can enable active targeted delivery to metastatic LNs (Fig. 3C). Recognizing the imaging potential of DDSs, researchers have committed themselves to the development of LNM imaging using DDSs. This aims to enhance the efficiency and precision of diagnosing cancer LNM through the introduction of this delivery system (Fig. 3).

Current techniques in LN imaging

Several methods for lymphatic imaging are available, enabling visualization of LN structures in various body parts and diagnosing LNM. The minimal density difference between LNs and surrounding tissues, however, often complicates the diagnosis of metastasis through imaging, leading to misdiagnoses and missed diagnoses [78]. Frequently, contrast agents are employed to enhance the imaging effect and improve tissues contrast. Although many articles detail non-targeted and traditional LN imaging techniques, this section focuses on the principles and limitations of imaging agents within these traditional administration methods [79]. This coverage encompasses numerous imaging techniques employed in medical diagnostics, such as X-ray scans and digital imaging methods.

Digital imaging techniques, such as CT, MRI, US imaging, NIR lymphography, and other LN imaging techniques, have revolutionized the medical field by enabling high contrast, high resolution, and minimally invasive LN imaging [80–82]. Despite these advancements, traditional administration methods paired with various imaging techniques, while offering acceptable results, continue to face issues such as lack of targeting, brief fluid retention time, and limited detection points. These drawbacks inhibit the effectiveness of diagnosing LNM [83, 84].

X-ray imaging

The earliest approach to LN imaging involved the use of X-rays to visualize LNs post the injection of contrast agents [85]. However, this method necessitates invasive contrast agent injections, conflicting with modern non-invasive diagnostic philosophies and negatively impacting patient compliance [86].

LSG and SPECT/CT

LSG, recognized as the gold standard for LN imaging, is routinely employed to assess lymph transport and identify metastatic LNs associated with cancer [39]. This procedure encompasses the administration of a tracer, imbued with a radioactive isotope, into interstitial tissues. Subsequently, a single-photon-emission-computed-tomography (SPECT) instrument external to the body is utilized to monitor the tracer's path.

Coupling LSG with SPECT/CT facilitates three-dimensional imaging of the lymphatic system, thereby accurately locating metastatic LNs [87, 88]. This combined approach, when utilized with DDSs, proves instrumental for the precise localization of the SLN and for effectively guiding LN biopsy in breast cancer patients [89].

Dilege et al.'s study indicated that this imaging methodology was able to accurately identify all sampled LNs. Notably, 88.5% of the patients' clipped nodes were classified as SLN in this study. This enables early detection and precise excision of metastatic LNs, thus mitigating the likelihood of postoperative complications [90].

However, there exist limitations with non-NP-based Technetium-99 (99mTc) complexes, commonly employed in this context. Shortcomings such as a brief half-life and suboptimal contrast degrade the diagnostic value of the resultant imaging.

PET/CT

Glucose serves as the principal energy source for human cells. Exploiting the Warburg effect, cancer cells hinder the tricarboxylic acid cycle and preferentially use the glycolytic pathway for energy provision, albeit with lower efficiency. Consequently, malignant tumors display a markedly higher uptake of glucose compared to normal tissues [91].

Positron-emission-tomography (PET)/CT leverages this distinct trait of malignant tumors by employing radiolabeled glucose analogs as tracers to image pathological tissue. Herbrink et al., for instance, utilized 18F-fluoro-deoxyglucose (18F-FDG) as a tracer to investigate LNM in patients diagnosed with non-small cell lung cancer, achieving an accuracy rate of 81% [92]. Similarly, Billé et al. employed 18-FDG to detect LNM in a cohort of 159 non-small cell lung cancer patients, documenting a specificity of 91.9% and an accuracy rate of 80.5% [93].

Nevertheless, FDG-PET/CT has exhibited limited sensitivity in detecting LNM in cases of esophageal squamous cell carcinoma, with a range of merely 30–40%. This could potentially result in false negative diagnoses [94, 95]. Furthermore, certain diseases may confound the diagnosis of metastatic LNs via FDG-PET. For instance, nodular lymphoid hyperplasia of the lung, a benign, non-neoplastic lesion, can manifest as multifocal lesions bilaterally, and its FDG-PET results can be falsely positive, potentially leading to misdiagnosis [96, 97]. Additionally, Manta et al. performed an FDG-PET/CT scan on a patient suspected of having thyroid malignancy. The results revealed a strong FDG uptake in the mediastinal and bilateral hilar LNs. However, post-surgical excision, the pathological examination revealed non-necrotizing granulomatous lesions, indicative of thyroid nodule disease [98]. This misdiagnosis could potentially prompt incorrect treatment strategies, thereby inflicting undue trauma on the patient.

MRI

MRI operates by inducing alignment of hydrogen atoms within the body using a magnetic field. The subsequent emission of radio waves following disturbance is captured and processed by an advanced computer system, culminating in the generation of detailed images depicting diverse tissues and other critical anatomical structures [99, 100].

Gadolinium-based contrast agents (GBCAs), such as Gd-DOTA, Gd-DTPA, are presently employed extensively for contrast-enhanced MRI. Owing to its strong paramagnetism, Gadolinium (Gd) influences tissue contrast by stimulating the relaxation of nearby hydrogen protons, facilitating indirect imaging [101, 102]. A study demonstrated that post-injection of Gd-DTPA, MRI yielded a sensitivity of 91.1% and accuracy of 87.2% in detecting metastatic LNs in patients with nasopharyngeal carcinoma. Precise and efficient localization of the SLN substantially mitigates unnecessary tissue resection, lessens surgical side effects, and enhances patient quality of life [103].

However, GBCAs are associated with certain drawbacks. Firstly, GBCAs exhibit potential cytotoxicity. Research has revealed that this contrast agent incurs nephrotoxicity in patients with chronic kidney disease, potentially resulting in nephrogenic systemic fibrosis. Secondly, the excretion of GBCAs poses a challenge. Even in patients with a normal glomerular filtration rate, the use of GBCAs can lead to gadolinium deposition in multiple organs. Certain patients may manifest symptoms such as skin burning pain, muscle cramps, and 'brain fog', indicative of gadolinium deposition disease [104–106]. As Gd can persist in the brain for prolonged periods, the

FDA has issued a warning about “GBCA retention in the body” [107], and the European Medicines Agency (EMA) has classified GBCAs as a high-risk imaging agent [108].

NIR fluorescence imaging

NIR fluorescence imaging technology, following the administration of a fluorescent dye, stimulates the fluorescent properties of this dye through a detector, thus facilitating visualization the contrast agent and enabling LN imaging. Within the NIR spectrum, human tissue does not exhibit autofluorescence, thus yielding high contrast favorable for imaging and observation [109]. Additionally, given that NIR light is invisible, the use of this fluorescent dye minimizes visual impact on patients, thereby reducing potential negative emotional responses [110].

ICG, a contrast agent approved by the FDA for clinical use [41], boasts robust tissue penetration capacity attributable to its excited fluorescence (compared to traditional blue dyes, which are easily obscured by dense tissues like fat, leading to inadequate imaging depth [111]), superior biocompatibility, and non-radioactive properties [112]. ICG has been broadly utilized in NIR fluorescence imaging [113, 114], offering real-time and accurate detection of metastatic LNs [115–117].

But there are certain drawbacks associated with ICG that compromise the efficacy of LNM imaging. Firstly, ICG’s amphiphilic properties and poor stability in aqueous solutions lead to aggregate and self-quenching in body fluids, thereby inhibiting the ability of imaging agents to reach the LNs [118]. Secondly, ICG’s low molecular weight hampers its retention in the SLN, resulting in potential drainage to other LNs or clearance via blood vessels, thus reducing imaging specificity [119]. Moreover, the first NIR window (NIR-1) (700–900 nm) is impacted by signal scattering of biological endogenous substances, resulting in excessive background signal in the image and inadequate tissue contrast, which compromises image-based diagnosis [120, 121].

Additionally, the toxicity of ICG correlates with light duration [122], indicating that the effectiveness of LNM detection using ICG hinges on the physician’s expertise and technical acuity. This could potentially lead to a disparate distribution of medical resources and unequal access to medical diagnosis and treatment for patients. Therefore, the redefinition of LNM diagnostic principles and strategies is pivotal, not only to enhance survival and quality of life for cancer patients but also to promote social equity.

US imaging

US imaging operates on the principle of sound wave reflection. It gathers these reflected sound waves from

tissue organs and converts them into images [123]. Some researchers have attempted to augment the contrast of US imaging using microbubbles (size < 10 μm) encapsulating diagnostic gas, thereby procuring high spatial-temporal resolution images. However, their constrained contrast and indistinct tissue boundaries may compromise the diagnostic accuracy for LNM [22, 124].

DDSs for targeting and imaging of LNs

In recent decades, the use of DDSs has expanded considerably. These systems find widespread application in drug delivery, tissue engineering, and medical imaging, among other fields [125–127]. Particularly within the realm of LN imaging, scholars have begun investigating DDSs due to their characteristics of reducing toxicity and enhancing action, aiming to overcome the limitations of traditional imaging methods and agents. A large number of studies have demonstrated the effectiveness of DDSs in LNM imaging [128–131]. Specifically, DDSs based on NPs possess unique characteristics of a high surface area-to-volume ratio, which can achieve strong and longitudinally stable imaging signals. By reducing the unexpected reaction between the drug and the body’s microenvironment, controlling drug release, and altering biological distribution, the toxic and side effects of the contrast agent on the body can be minimized. Secondly, the strategy of active and passive targeted delivery of DDSs can detect the desired target and improve the sensitivity and specificity of imaging. Additionally, DDSs can protect the drug from degradation in the body, improve the drug’s bioavailability, and ultimately achieve the purpose of reducing toxicity and increasing efficiency [132]. Various forms of DDSs, such as wafers, foams, films, hydrogels, NPs, and fibers, have been developed [133–138]. Among them, NPs are the most popular in the realm of LN imaging and can be roughly classified into lipid NPs, radioactive nano-colloids, metal NPs, magnetic NPs, etc. [139–142]. Available preparation methods include self-assembling systems, microfluidic production, aqueous coprecipitation, thermal decomposition, sol–gel reaction, etc. [132, 143, 144].

Depending on the disease, the desired effect, and the characteristics of the drug, the route of administration of DDSs can usually be divided into oral, parenteral, transdermal, and nasal administration, among others [145]. Parenteral administration is currently the most commonly used invasive route of DDS administration, with advantages including bypassing first-pass metabolism, rapid onset, controllable drug utilization, reduction of gastrointestinal irritation, and reliability for critically ill patients. Parenteral administration can further be divided into subcutaneous, intramuscular, and intravenous injection, with the absorption and onset rate of

Table 1 Imaging technologies based on drug delivery systems (DDSs)

Imaging technologies	Principle	Example of DDSs	Advantages	Refs.
LSG and SPECT/CT	Injecting a tracer containing a radioactive isotope into the interstitial tissues and using external detection instrument (SPECT) to track and image it	99mTc-labeled nanocolloid DDSs (99mTc-sulphur colloid, 99mTc-nanocolloidal albumin, 99mTc-antimony trisulfide colloid, 99mTc-etarfolatide, etc.)	The short half-life and poor contrast of the 99mTc complex are improved; Helping in the early detection of SLN; Guiding lymph node biopsy effectively; Reducing the occurrence of postoperative sequelae, etc	[147, 149–151]
PET/CT	Tumor tissues exhibit abnormally increased glucose uptake. PET/CT utilizes radiolabeled glucose analogs as tracers to image the lesion tissue based on this characteristic of malignant tumors	68 Ga-labeled targeted PSMA-DDS; 124I-labeled antibody against LVE-1 DDS	Increasing the sensitivity and accuracy of diagnosis and reducing the occurrence of misdiagnosis and missed diagnosis; Improving the targeting of imaging agents to lymph nodes, etc	[167, 168]
MRI	MRI uses strong magnetic fields and radio waves to create detailed images of the body's internal structures. The magnetic field aligns the body's protons, and the radio waves cause them to emit signals which are detected and analyzed to create images	Gd ₂ O ₃ PCD coated DDS; USPIO DDSs	Reducing Gd deposition and cytotoxicity; Pharmacokinetics and biocompatibility are satisfactory; Having higher diagnostic specificity and sensitivity, etc	[171, 172, 174]
NIR fluorescence imaging	NIR fluorescence imaging technology is used to visualize lymph nodes. It involves injecting a fluorescent dye and exciting its fluorescent properties using a detector to create contrast agent visualization	PLGA-ICG DDSs; γ-PGA-ICG DDSs; PEG coated ICG-DDSs; Metal nanoclusters DDSs	Good retention rate and stability in vivo; Having a stronger NIR fluorescence signal than ICG; Increasing the molecular weight to reduce clearance by blood; Serviceable tissue penetration and lower interference signals from endogenous substances, etc	[111, 180, 188, 190]
US/PA imaging	US imaging is based on the principle of sound wave reflection, collecting the reflected sound wave from the tissue organs and converting them into images. PA imaging uses laser-generated light pulses to generate acoustic waves in the body's tissues which are detected and analyzed to create images	Carbon NP DDS; Cu-neodecanoate DDS	Satisfactory SLN imaging capability, imaging depth, signal noise, ratio and tissue contrast, etc	[194–196]
Multimodality imaging	Combining different lymph node imaging technologies	GC-AuNCs/ICG DDS (PA/Fluorescence imaging); Nanoprobes DDSs (PA/Fluorescence imaging); Iron oxide-ATF DDS (NIR/PA/MR I)	To compensate for the limitations of different technologies, take advantage of each technology. Explore the potential of lymph node imaging technology based on DDSs	[198–201]

LSG lymphoscintigraphy, SPECT single-photon-emission-computed-tomography, CT computed tomography, DDSs drug delivery systems, SLN sentinel lymph node, PET positron-emission-tomography, PSMA prostate-specific membrane antigen, LVE-1 lymphatic vessel endothelial hyaluronan receptor-1, MRI magnetic resonance imaging, USPIO ultrasmall superparamagnetic particles of iron oxide, NIR near-infrared, PLGA poly (DL-lactic-co-glycolic acid), ICG indocyanine green, PEG polyethylene glycol, US ultrasound, PA photoacoustic, NP nanoparticle, ATF amino-terminal fragments

the drug increasing respectively [146]. At present, DDSs used in LNM imaging can be roughly divided into two methods: one is to increase the efficiency of delivery (e.g., ^{99m}Tc-labeled colloids), and the other is to increase the specificity of delivery (such as surface modification with tumor antigen ligands). This paper will categorize various imaging techniques that utilize DDSs and present them in tabular form (Table 1). In the following sections, we will review the delivery system represented by NPs.

LSG and SPECT/CT

In LSG, the controlled administration strategy most frequently utilized involves NP-colloid-based DDSs labeled with the radioactive isotope ^{99m}Tc. This approach mitigates concerns associated with short half-lives and sub-optimal contrast. An example is ^{99m}Tc-etarfolatide, a DDS carrying a ^{99m}Tc-labeled folate conjugate, designed for imaging targeting folate receptors on tumor cells. Preclinical studies have shown that ^{99m}Tc-etarfolatide has a higher affinity with human folate receptors, thus improving the specificity of imaging [147, 148]. Drawing on the inherent spatial characteristics of NP carriers [24], a diverse range of ^{99m}Tc-labeled DDSs are currently in use, distinguished by the differing particle sizes of their NP carriers. For instance, ^{99m}Tc-sulfur colloid (particle size exceeding 100 nm) [149], ^{99m}Tc-nanocolloidal albumin (particle size less than 80 nm) [39, 150], and ^{99m}Tc antimony trisulfide colloid (particle size between 3 and 30 nm) [151].

The capacity for passive targeting of LNs by DDSs is determined by a variety of factors [152, 153], of which the particle size of NP carriers emerges as the most significant in LSG LN imaging [154, 155]. Particle sizes of less than 10 nm expedite clearance of DDSs from the interstitial fluid and allow for entry into the LN via the lymphatic vessel wall. However, such small particles can also easily traverse capillaries and thus be cleared prematurely. Conversely, DDSs with particle sizes greater than 200 nm are more likely to remain entrapped in the interstitium and be eliminated by the RES. The optimal particle size for DDSs, therefore, typically ranges from 10 to 100 nm. This range allows for broad and effective aggregation within metastatic LNs [155–158]. However, no consensus has been reached regarding the most suitable particle size range for DDSs [159, 160].

DDSs with an appropriately sized particle can achieve significant regional LN retention. This facilitates intraoperative positioning via a γ probe and allows for accurate and repeatable SLN localization [161, 162]. This precision reduces the need for radical LN dissection surgery. It is crucial to remember, however, that radioactive isotopes possess inherent decay properties. Therefore, the

attenuation correction of results is indispensable to ensure accuracy [163].

PET/CT

The conventional radiolabeled tracers, epitomized by ¹⁸F-FDG, although possessing high sensitivity and specificity in detecting tumor metastasis, present significant limitations, consequently lowering diagnostic accuracy and restricting their diagnostic value. Due to the non-targeted nature of traditional contrast agents, the potential toxicological side effects of imaging agents during the diagnostic process are particularly prominent. Moreover, the non-targeted feature restricts the accuracy of diagnosis and the ability to distinguish small lesions. These shortcomings underscore the need for an altered administration approach, one that promises enhanced sensitivity and precision.

Recent studies have begun to employ surface-modified DDS tracers for LN imaging, a technique that facilitates the entry of DDSs into LNs and enhances the targeting of imaging agents [164–166]. Schilham et al. utilized tracers based on ⁶⁸Ga-labeled targeted prostate-specific membrane antigen (PSMA) DDS, injecting these into patients with prostate cancer to detect LNM. The modified PSMA DDS demonstrated superior sensitivity to LNM compared to ¹⁸F-FDG, with diagnostic accuracy reaching up to 85% [167].

In another study, Mumprecht administered a ¹²⁴I-labeled antibody against the lymphatic vessel endothelial hyaluronan receptor-1 (LYVE-1) DDS to mice carrying the B16-F10-luc2-VEGF-C tumor with LNM [168]. These surface-modified, immunotargeted DDSs showed heightened sensitive to LNM compared to ¹⁸F-FDG [169], accumulating in high concentrations at specific sites within LNs. This undoubtedly yielded significant improvements in the diagnostic accuracy of PET-CT [170].

MRI

Although MRI plays a significant role in displaying soft tissue imaging, the side effects of GBCAs might not be acceptable to clinical doctors and patients. The deposition of GBCAs in the brain could lead to symptoms related to central nervous system toxicity or neuroinflammation, which has been a particular concern for the EMA [103, 106]. To address the aforementioned challenges associated with GBCAs, several studies have successfully incorporated DDSs into magnetic resonance LN imaging, yielding substantial improvements. One such strategy involved modifying Gd with polycyclodextrin (PCD) to generate a Gd₂O₃PCD-coated DDS. When applied to a mouse model of breast cancer, this system demonstrated the capability to deliver GBCAs at

lower dosage requirements, thereby enhancing imaging localization of LNM. Thanks to the Gd-modified coating, which effectively reduced Gd leakage and required lower concentrations, this DDS can decrease Gd deposition and cytotoxicity. This reduction mitigates the side effects associated with detection and enhances the biosafety of imaging [171]. Further to this, ultrasmall superparamagnetic particles of iron oxide (USPIO) currently represent the most extensively studied and utilized NPs for MRI [172–175]. Ferumoxtran-10, a type of USPIO, presents wide-ranging application prospects [176]. This compound is absorbed by macrophages, targeted, and transported to LNs where it is primarily distributed [177]. With satisfactory pharmacokinetics and biocompatibility, it proves suitable for MRI imaging detection of human LNs [178, 179]. Importantly, the use of USPIO-based DDSs for LNM detection demonstrates higher diagnostic specificity and sensitivity compared to MRI detection techniques not based on DDSs. Koh DM et al.'s research showed that, compared with non-DDS-based imaging diagnosis, LNM detection using DDSs based on USPIO shows higher diagnostic specificity, with an average specificity increase from 75 to 93% [175].

NIR fluorescence imaging

ICG forms aggregates in body fluids and lacks stability in aqueous solutions, which hinders its effective delivery to LNs. Its low molecular weight results in poor retention in SLNs, thus reducing imaging specificity. Moreover, the NIR-I window also suffers from signal scattering and excessive background noise, which can undermine diagnostic accuracy [119]. To surmount the constraints of ICG in NIR LN imaging, researchers have sought to employ DDSs to enhance ICG delivery. DDSs, such as ICG encapsulated with poly (D,L-lactic-co-glycolic acid) (PLGA), showed a release of 78% of the encapsulated ICG within the initial 8 h of bodily introduction, with the residual portion being discharged in the subsequent 16 h. Compared to its unencapsulated counterpart, ICG-NaI, PLGA-ICG demonstrated an eight-fold increase in retention rate [180].

Poly (γ -glutamic acid) (γ -PGA)-ICG DDSs also showcase promising features. They display notable stability in an aqueous solution, resist aggregation and self-quenching at physiological temperatures, and produce a more robust NIR fluorescence signal than conventional ICG. The augmentation of their molecular weight aids in diminishing blood clearance, thereby enhancing their targeted delivery capacity to LNs and improving the imaging capabilities for LNM [111].

Modifying ICG DDSs with polyethylene glycol (PEG) polymers may also mitigate the adverse effects of ICG on LN contraction and dilatation [111, 181]. In addition to

advancements in imaging materials for the NIR-I window, continuous efforts are underway to develop materials for the second NIR window (NIR-II) (1000–1700 nm). This development aims to address the shortcomings of NIR-I imaging, focusing on achieving superior tissue penetration with less signal interference from endogenous substances and improving imaging contrast [182, 183].

In this regard, metal nanoclusters have piqued researchers' interest due to their unique attributes. As nanomaterials with a particle size ranging 1–40 nm, they exhibit distinctive surface plasmon resonance (SPR) characteristics with high adjustability [184, 185]. Notably, gold is extensively utilized in the development of nanocluster-based DDSs due to its excellent biocompatibility, size adjustability, and surface treatment capabilities [186].

By altering the structure and composition of gold nanocluster-based DDSs, the SPR position can be modified. If the SPR peak is situated in the 700–900 nm region, it can serve as a NIR-I fluorescence imaging contrast agent [187]. Conversely, when the SPR peak of gold nanocluster-based DDSs is set at 1000–1700 nm, these DDSs function as a NIR-II imaging agent, whose long-wavelength, low-scattering properties permit photons to penetrate deep tissue [188]. Research has revealed that the imaging depth of NIR-II imaging using gold nanoclusters can extend to 6.1 mm subcutaneously, a marked improvement from the 5 mm depth achieved by ICG [189]. This approach also offers high stability, sensitivity, and superior imaging resolution [190, 191].

Further enhancements to gold nanoclusters were made by incorporating targeting molecules, thus endowing the gold nanoclusters with specificity for SLN imaging. These gold nanoclusters were then modified with sulfhydryl ligands targeting DCs. Following injection of this DDS into mice, a significant accumulation in metastatic LNs was observed. This greatly enhanced imaging specificity and markedly improved the ability to identify LNM [192].

US/PA imaging

Efforts have been made by researchers to enhance the efficacy of acoustic imaging through the exploitation of the photoacoustic (PA) effect. When human tissue absorbs and subsequently releases pulsed lasers, this expansion and contraction process generates US waves. Since different tissues absorb light to variable extents, this results in the production of US waves with differing intensities [193].

In integrating the properties of PA and US, researchers have achieved PA/US dual-mode imaging, utilizing optical excitation and acoustic detection. This approach leverages the unique attributes of the nanomaterial carriers used DDSs [31]. For instance, the specific spatial

size effect of carbon NP-based DDSs allows for facilitated entry into the lymphatic system [23]. While macrophages in healthy LNs can clear these DDSs, metastatic LNs, infiltrated by cancer cells, exhibit a significant decrease in macrophages, which results in reduced DDS uptake.

Owing to these properties, carbon NP-enhanced PA/US LN imaging offers superior SLN imaging capability, along with improved PA/US imaging depth, tissue contrast, and signal noise ratio. This technique thus demonstrates higher recognition and diagnostic capabilities for LNM compared to conventional US imaging [194]. Furthermore, carbon nanomaterial-enhanced PA imaging can achieve a greater penetration than NIR imaging based on ICG, reaching an imaging depth of over 12 mm [195].

Dipanjan et al. proposed an advanced strategy in which they mixed polystyrene and Cu-neodecanoate complexes, coating the resultant mixture with phospholipids to enhance imaging. This DDS exhibits a broad light absorption spectrum and provides exceptional PA contrast within NIR-I. It is noteworthy that this DDS effectively circumvent to toxicity of copper when applied in vivo, thereby suggesting a potential role for copper as a cost-effective material in future LNM imaging [196].

Multimodality imaging

Although each of the above-mentioned imaging methods has unique advantages, they also possess certain defects that limit the ability to obtain reliable and accurate information. Combining two or more imaging modes into one system can produce more accurate imaging details than traditional imaging methods. An ideal strategy to enhance the accuracy and specificity of cancer diagnosis has emerged by coupling various LN imaging modalities, such as NIR fluorescence imaging, US imaging, and PA imaging. This multimodal imaging strategy yields a more comprehensive representation of the lymphatic system, facilitating the detection of a greater number of anomalies. Consequently, doctors can devise more efficacious treatment plans for cancer patients by integrating multiple imaging technologies.

The aforementioned enhancement of PA/US imaging through the utilization of carbon NP-based DDSs exemplifies this integrated imaging approach. Certain researchers have amalgamated the high specificity of PA imaging with the high sensitivity of fluorescence imaging to counteract the limited imaging depth of fluorescence imaging and the reduced sensitivity of PA imaging [197]. Serving as a “bridge” between two distinct imaging techniques, the gold nanocluster with PEGylated chitosan coating and ICG mixture (GC-AuNCs/ICG) in the DDS plays a role in the combined imaging technology, operating synergistically and without mutual interference,

thereby leveraging the benefits of both imaging techniques [198].

In another study, researchers employed a DDS to deliver PA and fluorescence dual-modal nanoprobe for experimental studies on mouse models of breast cancer [199]. The high spatial resolution and depth of 3D information supplied by preoperative PA imaging were utilized to locate the primary lesion and guide tumor excision. During the procedure, the high sensitivity of NIR fluorescence imaging was harnessed to map suspected residual lesions and metastatic LNs in the vicinity of the surgical area for secondary resection [200]. Pathological analysis post-surgery revealed that over 70% of the secondary resection specimens confirmed the presence of tumor cells with the aid of fluorescence imaging. Following surgery guided by PA/fluorescence combined imaging technology, the local recurrence rate in the mouse model was 0 after 30 days, significantly lower than the 33.3% local recurrence rate observed in the control group.

Apart from PA/fluorescence combined imaging, Yang et al. coupled iron oxide with amino-terminal fragments (ATFs) to formulate a DDS for NIR/PA/MR combined imaging in mouse models of pancreatic cancer [201]. This DDS was capable of specifically delivering its contents to the target LN. In vivo combined imaging demonstrated that optical imaging can accurately locate the primary tumor and multiple metastases, and MRI providing high-resolution imaging of the lesions following localization, offering rich anatomical details [202]. Such high-resolution imaging data prove advantageous for surgeons, allowing for a detailed understanding of the lesions and avoidance of damage to adjacent tissues. The specific binding of the targeted multimodal imaging mode enhances the selective accumulation of the imaging agent at the target, making the diagnosis more accurate. The evolution and advancement of DDS-based multimodal imaging modes have significantly contributed to the localization of LN metastases, reduced surgical trauma, and generated novel insights for the future progression of LN imaging technology [203].

Integration of diagnosis and treatment in DDSs

Post precise diagnosis, surgical resection stands as the primary treatment modality for cancer and LNM, with radiotherapy and chemotherapy acting as supplementary or adjunctive therapies during the treatment process. Traditional radiotherapy and chemotherapy, however, lack specificity and may engender adverse effects on normal tissues, thereby impacting overall health [204]. Substantial research has indicated that DDSs, owing to their high targeting and customization capabilities, are efficacious in delivering imaging agents or therapeutics

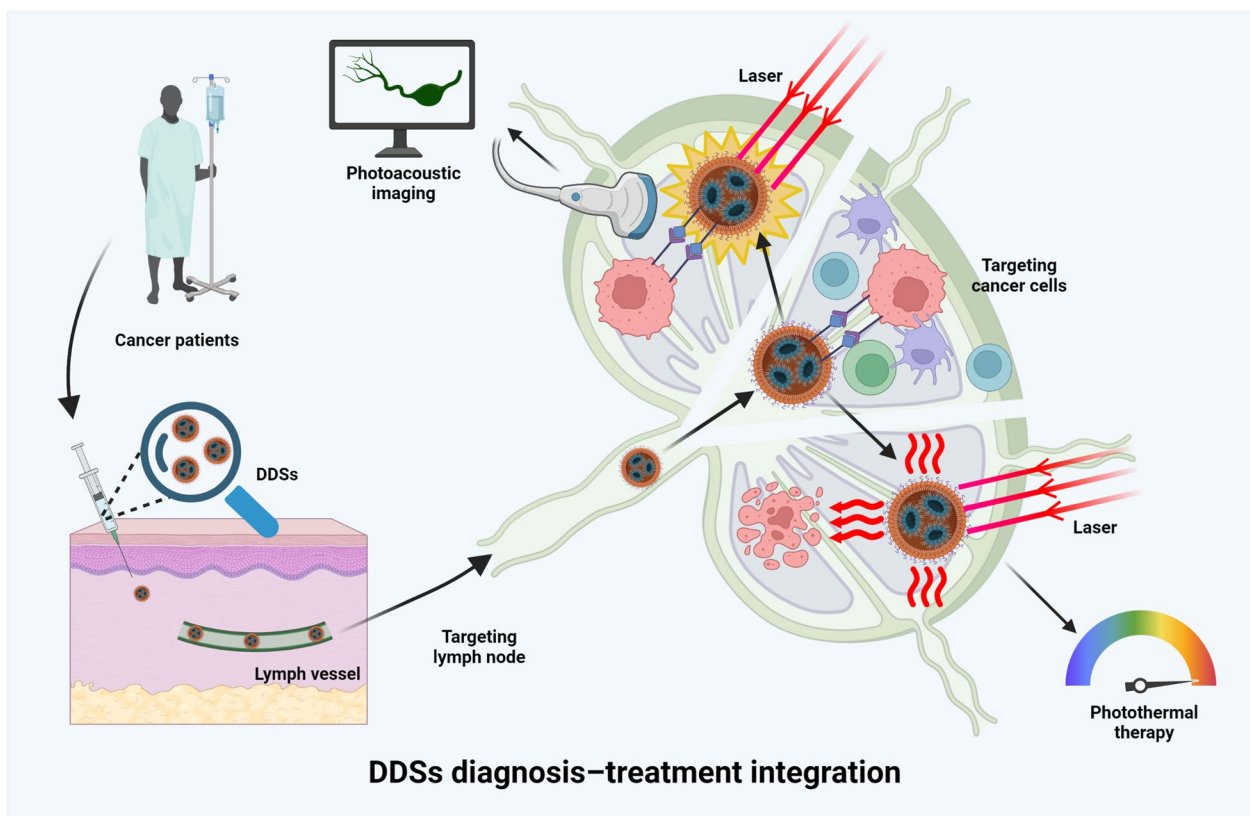


Fig. 4 The dual role of drug delivery systems (DDSs) in diagnosis and treatment, demonstrating the application of DDSs in delivering photothermal agents. These agents convert light energy into photoacoustic signals for imaging, while simultaneously releasing thermal energy, derived from light absorption, to annihilate tumor cells. Created with BioRender.com

[164, 205–210]. Hence, researchers have endeavored to amalgamate the diagnostic and therapeutic functions of DDSs.

Among the multitude of integrated diagnosis-treatment approaches, photothermal therapy (PTT) has been garnering considerable attention. Given that tumor cells exhibit lower heat tolerance than normal cells, PTT capitalizes on this property to eradicate cancer cells by generating heat energy through the photothermal conversion of photothermal agents under irradiation at specific wavelengths [211]. Prussian blue DDSs, with their excellent biocompatibility, photothermal conversion efficiency, and absorption range within the NIR window, prove to be an optimal choice for PTT and PA imaging. Upon laser exposure, Prussian blue DDSs convert light energy into PA signals for PA imaging, while concurrently releasing the thermal energy converted from light absorption to exterminate tumor cells [212]. Nevertheless, this thermal ablation treatment modality lacks targeted capability towards lesion areas, and may induce damage to adjacent tissues if the temperature is excessively high [213], thereby diminishing patients' quality of life. This shortcoming limits the clinical application

and therapeutic efficacy of PTT; hence, it is necessary to improve the targeting of PTT and reduce the side effects of treatment [214]. Building on the high expression of the CD44 molecule in cancer cells [77], researchers have coated the CD44 ligand, hyaluronic acid (HA), onto DDSs loaded with chemotherapeutic drugs. This strategy actively transports diagnostic and therapeutic agents by targeting cancer cells rich in CD44, thereby significantly enhancing the targeting of imaging agents and decreasing the damage of PTT to the surrounding tissue [214]. Such a DDS achieves the integration of diagnosis and treatment for LNM by concurrently enabling imaging, PTT, and targeted transport of chemotherapeutic drugs under 1000–1700 nm second NIR window laser exposure. Initial drug delivery by DDSs is marked by a clear and stable NIR imaging signal; as PTT and chemotherapy drugs gradually inflict damage to tumor cells, the NIR signal significantly diminishes, which further confirmed its effect (Fig. 4).

Apart from PTT and the delivery of conventional chemotherapy drugs, DDSs can also actualize diagnostic and therapeutic effects in other ways. For instance, Yang et al.

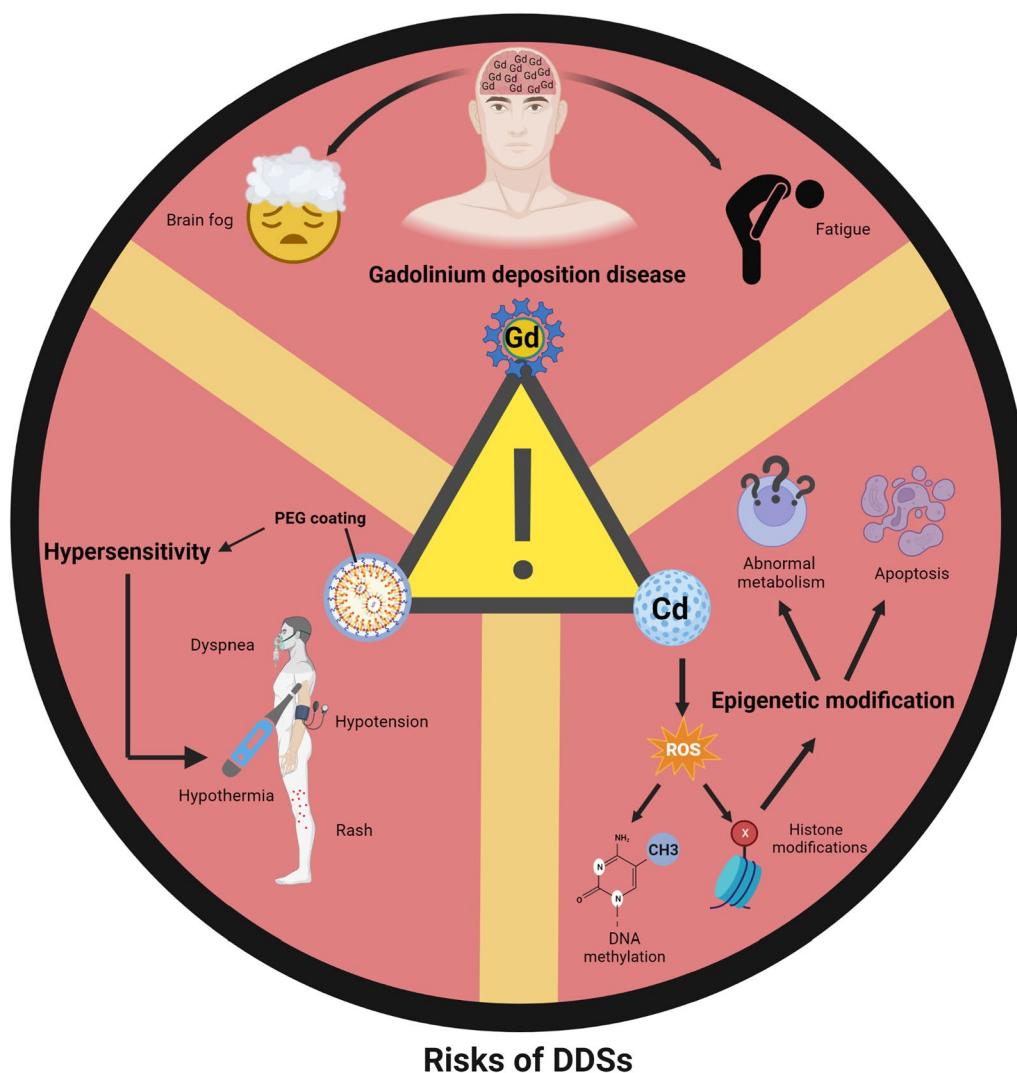


Fig. 5 The potential risks associated with drug delivery systems (DDSs) in the context of lymph node metastasis imaging. Nanoparticle (NP)-based DDSs are not devoid of safety concerns. For instance, DDSs containing Gd may precipitate gadolinium deposition disease, causing symptoms such as fatigue and brain fog. Quantum dot-based DDSs may induce the production of reactive oxygen species (ROS) via the release of metal ions, such as the Cd ion, resulting in epigenetic modifications. Despite its initial status as an ideal, safe coating to mitigate DDS side effects, polyethylene glycol (PEG) might still instigate hypersensitivity reactions. Created with BioRender.com

synthesized a high-affinity ligand for the urokinase plasminogen activator receptor. When coupled with a carrier, this ligand can inhibit tumor growth by competitively blocking the binding of natural ligands to receptors while also imaging regional LNM in pancreatic cancer [201]. Additionally, research on nano-microbubbles-based DDSs in integrated diagnosis-treatment approaches has also garnered interest. Utilizing US waves, microbubble oscillation is induced to enhance the ultrasonic contrast of the target site. Gases present in microbubbles, such as dioxygen, NO, and CO, can modify the tumor microenvironment, thereby generating therapeutic effects [215–217]. There is no doubt that although surgery is the main

treatment for LNM, the concept of integrating diagnosis and treatment through DDSs provides a new idea for the minimally invasive and precise treatment of LNM. The diagnostic and therapeutic model based on DDSs harbors immense potential for clinical application.

Challenges and prospects

As previously delineated, LN imaging predicated on DDSs may alleviate the toxic side effects of traditional contrast agents and enable the targeted transport of chemotherapy drugs within an integrated diagnosis and treatment model, thus reducing damage to normal cells [106, 122, 218]. The development and research of

DDSs have advanced significantly; however, the potential for clinical transformation of DDSs remains limited. Although the global nanomedicine market was valued at \$242.6 billion, with 563 nano-based DDS products in various stages of clinical trials or development in 2021 [219], only about 100 nanomedicines have actually been commercialized. Factors such as toxicity, high costs, and unclear regulatory guidelines have emerged as substantial barriers to their clinical application [220]. The risks associated with DDSs predominantly pertain to metabolic and toxicity factors, as well as a lack of standardization, presenting challenges for the application and transformation of DDSs (Fig. 5).

Metabolism of DDSs

Typically, upon systemic introduction, DDSs accumulate, albeit to a certain extent, in various anatomical structures such as LNs, heart, spleen, and kidneys via fluid distribution, and are subsequently excreted through diverse pathways, thus avoiding significant bodily accumulation [221–223]. Contrarily, certain studies have found that some DDSs may persist within the body and prove challenging to effectively eliminate, thereby engendering side effects [224, 225]. Not only in the brain, but studies have also found that NPs can pass through biological barriers, deposit in the reproductive system, and cause damage to germ cells [226–228]. Studies have shown that plasma proteins adsorb onto the surface of NPs, altering their properties (such as size, shape, surface charge) and leading to abnormal protein aggregation and folding. This subsequently causes the NPs to off-target, reducing drug utilization, and leading to accumulation [229]. The development and use of modified coatings, such as PEG, will be very helpful. In addition, the metabolic characteristics of common abnormal accumulation organs such as the kidneys, liver, and brain need to be further studied, and the interactions between DDSs and these organs need to be explored.

Toxicity of DDSs

Despite the great strides made in biosafety, DDSs still pose hidden dangers of toxicity [230]. DDSs based on quantum dots can stimulate the production of reactive oxygen species (ROS) through the release of metal ions, such as Cd ions [231]. This process can disrupt cellular metabolism [232], inflict DNA damage [233], and ultimately precipitate cell apoptosis [234]. Furthermore, the pro-oxidation properties of DDSs may elicit epigenetic alterations by interfering with RNA and chromatin remodeling [235]. Examples of such interactions include gold NPs influencing the activity of histone deacetylase

[236] and superparamagnetic iron inducing high acetylation of core histones [237].

To imbue DDSs with safety, inertness, and stability, the carrier portion can be modified via PEGylation. PEG is considered a non-immunogenic material, which not only mitigates the interaction between the DDS core and the biological milieu, thereby enhancing safety [171, 238], but also bestows DDSs with stealth effects, diminishes protein adsorption, and precludes cellular ingestion, thus extending circulation time. Therefore, PEG was once widely considered an ideal and safe strategy to reduce the toxicity of DDSs [239–242]. Regrettably, a small amount of evidence suggests that PEG can trigger hypersensitivity reactions [243–245], manifesting symptoms such as respiratory distress, hypothermia, hypotension, rashes, and even mortality [246], thereby jeopardizing patient safety. Furthermore, it has been proven that the combination of PEG with protein or lipid NP materials can induce the body to produce anti-PEG antibodies, which often affect the distribution of PEGylated products and enhance their clearance rate, thus affecting the realization of the expected efficacy [247–250]. With the increasing application of PEG in cosmetics, food, medicine, vaccines, and other fields, the incidence of hypersensitivity reactions and the reduction of the efficacy of PEGylated drugs may increase [251]. At present, the mechanism of PEG-based DDS-induced hypersensitivity and anti-PEG antibodies is still uncertain. However, due to the widespread use of PEG, understanding its mechanism and solving adverse reactions is very important to obtain more effective preventive measures. Further development of modified coatings with low or no immunogenicity without compromising performance is warranted.

Delivery mechanism of DDSs

To achieve superior image quality, DDSs must rapidly infiltrate and accumulate in metastatic LNs. Despite ongoing research and innovation, the delivery efficiency of extant DDSs remains suboptimal. A retrospective analysis showed that only 0.7% (median) of the administered dose was delivered to solid tumors [252]. Previous studies have suggested that the tumor accumulation of DDSs is highly dependent on their size, based on the EPR effect [155, 253, 254]. As previously noted, excessively large DDS particle sizes impede LN entry, while exceedingly small particle sizes limit metastatic LN retention [154]. However, some studies have questioned the effectiveness of the EPR effect in the human body [255, 256]. Currently, there is no consensus on whether the EPR effect exists in the human body or the appropriate size range for DDS carriers [159, 257]. In the future, it is necessary to verify

the effect of EPR, focusing on exploring the accumulation, isolation, and clearance mechanisms of DDSs in the human body, as well as the interaction between DDSs and tumors, in order to further improve the delivery efficiency of DDSs.

Specificity of DDSs

To minimize side effects and extraneous organ distribution, DDSs should exhibit enhanced targeting of tumors and metastatic LNs. The existing targets for tumors and LNM do not fully meet the needs of accurate imaging, posing a hindrance to the clinical application of DDSs. The development of additional immune targets to augment the specificity of LN imaging, based on tumor characteristics and the metastatic LN microenvironment, might emerge as a prominent future direction [258–260]. With advancements in sequencing technology, clinical precision medicine has been greatly promoted [261]. Multi-omics analyses, such as genomics, metabolomics, and transcriptomics, are important means to identify therapeutic targets and molecular biomarkers currently and in the future, and to realize the personalization of cancer treatment [261–263]. In addition, the deep learning model based on radiomics and digital pathology also holds far-reaching significance for the mining of immune targets and imaging diagnosis [264].

Integration of diagnosis and treatment of DDSs

DDSs represent a method of administering imaging agents imbued with boundless potential. In the medical realm, DDSs have robustly validated their value in both imaging and drug delivery. Concurrent with the evolution of nanotechnology, the concept of “diagnosis-treatment integration” through DDSs has been proposed. This concept is capable of executing therapeutic functions while accurately locating lesions or metastatic LNs. The previously mentioned PA/PTT technology constitutes an initial realization of this concept. Nevertheless, it is important to note that multimodal imaging still has many shortcomings that need to be addressed by technological development, such as high cost, cumbersome imaging procedures, and the burden of high doses of imaging agents on the patient. Looking forward, we anticipate that DDSs can fully actualize their highly customized potential, achieving multifunctionality not only for diagnosis-treatment integration but also in becoming a “universal imaging agent and delivery system.” As a conduit linking various imaging technologies with their respective advantages, DDSs can enable the synergistic functioning of imaging technologies without burdening patients with the risk of multiple imaging agent injections.

Standardized risk assessment protocols

The dearth of standardized risk assessment protocols for DDSs constitutes a significant issue warranting collective attention, which may lead to patients receiving inappropriate treatment or missing the best treatment opportunity [265]. Regarding risks, researchers and clinicians may need to comprehensively explore the potential risks of DDSs applied to LN imaging, stratify these risks according to their likelihood and severity, and then establish a standardized treatment plan based on the corresponding risk stratification. Only by addressing these fundamental problems can we effectively promote the development and clinical transformation of DDSs. It is important to note that the Cancer Nanomedicine Repository provides a database that can determine the relationship between the physical and chemical properties of biological systems and NPs in real time, and analyze the delivery efficiency of DDSs [266]. Sharing and continuously analyzing experimental data is of positive significance for the clinical transformation of DDSs.

Such issues have considerably impeded the clinical adoption of DDSs. There is a need to promote the development of research, overcome the limitations of existing technologies, and develop DDSs that can effectively achieve the dual goals of reducing toxicity and increasing efficiency. Then, multi-stage preclinical and clinical trials should be performed. On the premise of ensuring biosafety, reducing costs and improving availability are necessary. The clinical transformation of the technology can ultimately be realized through the approval of relevant regulatory authorities.

Conclusions

The use of DDSs for imaging LNs presents an innovative approach in diagnosing LNM. The application of DDSs in LN targeting addresses several drawbacks associated with traditional, non-targeted drug delivery methods, notably by enabling precise localization within LNs. This precision enhances both the effectiveness and control of imaging agent delivery through multiple pathways. Consequently, it not only elevates the concentration of therapeutic agents in affected tissues but also significantly enhances the diagnostic accuracy for metastatic LNs. At the same time, this method allows for a reduction in the required effective drug dosage, thereby diminishing potential side effects [220]. Moreover, the coatings of DDSs can encapsulate imaging agents within their cores, thus precluding reactions with the biological environment and ameliorating biological distribution. This reduces bodily accumulation and consequently diminishes the toxicity of

imaging agents. Hence, employing DDSs to target LNs for imaging represents a nascent, promising technology. Although it necessitates further refinement and development for utilization in LNM diagnosis, the application of DDSs significantly enhances the accuracy of diagnosis, improves the success rate of surgery, reduces the incidence of surgical complications, and improves the quality of life of patients. There is no doubt that employing DDSs is an ideal LNM imaging.

Abbreviations

APC	Antigen-presenting cell
ATF	Amino-terminal fragment
CT	Computed tomography
DC	Dendritic cell
DDS	Drug delivery system
EPR	Enhanced permeability and retention
EMA	European Medicines Agency
FDA	Food and Drug Administration
GBCA	Gadolinium-based contrast agent
HA	Hyaluronic acid
ICG	Indocyanine green
LYVE-1	Lymphatic vessel endothelial hyaluronan receptor-1
LN	Lymph node
LNM	Lymph node metastasis
LSG	Lymphoscintigraphy
MRI	Magnetic resonance imaging
NIR	Near-infrared
NIR-I	The first NIR window
NIR-II	The second NIR window
NP	Nanoparticle
PA	Photoacoustic
PET	Positron-emission-tomography
PSMA	Prostate-specific membrane antigen
PLGA	Poly (D,L-lactic-co-glycolic acid)
PCD	Polycyclodextrin
PEG	Polyethylene glycol
ROS	Reactive oxygen species
RES	Reticular endothelial system
SPECT	Single-photon-emission-computed-tomography
SLN	Sentinel lymph node
SPR	Surface plasmon resonance
US	Ultrasound
USPIO	Ultrasmall superparamagnetic particles of iron oxide
PTT	Photothermal therapy
^{99m} Tc	Technetium-99
¹⁸ F-FDG	¹⁸ F-Fluorodeoxyglucose
γ-PGA	Poly (γ-glutamic acid)

Acknowledgements

Not applicable.

Author contributions

Ze-Min Cai: Conceptualization, Methodology, Investigation, Visualization, Writing—Original draft preparation, Writing—Reviewing and Editing. Zi-Zhan Li: Conceptualization, Methodology, Investigation, Writing—Original draft preparation, Writing—Reviewing and Editing. Nian-Nian Zhong: Methodology, Writing—Reviewing and Editing, Project administration. Lei-Ming Cao: Project administration, Writing—Reviewing and Editing. Yao Xiao: Validation, Supervision, Project administration, Writing—Original draft preparation. Jia-Qi Li: Validation, Investigation, Writing—Original draft preparation. Fang-Yi Huo: Conceptualization, Writing—Reviewing and Editing. Chun Xu: Supervision, Methodology, Writing—Reviewing and Editing. Bing Liu: Validation, Supervision, Writing—Reviewing and Editing. Yi Zhao: Supervision, Investigation, Writing—Reviewing and Editing. Lang Rao: Conceptualization, Methodology, Supervision, Funding acquisition, Writing—Review and Editing. Lin-Lin Bu: Conceptualization, Methodology, Supervision, Funding acquisition, Writing—Review and Editing. All authors have reviewed and approved the manuscript

for submission and agree to be accountable for all aspects of the work in ensuring that questions related to the accuracy or integrity of any part of the work are appropriately investigated and resolved.

Funding

This study was supported by Postdoctoral Science Foundation of China [Grant Numbers 2018M630883, 2019T120688], Hubei Province Chinese Medicine Research Project [Grant Number ZY2023Q015], Natural Science Foundation of Hubei Province [Grant Number 2023AFB665], Medical Young Talents Program of Hubei Province, and Wuhan Young Medical Talents Training Project to L.-L. B.

Data availability

No datasets were generated or analysed during the current study.

Declarations

Ethics approval and consent to participate

Not applicable.

Consent for publication

All authors are consent for publication.

Competing interests

The authors declare that they have no competing interests.

Author details

¹State Key Laboratory of Oral & Maxillofacial Reconstruction and Regeneration, Key Laboratory of Oral Biomedicine Ministry of Education, Hubei Key Laboratory of Stomatology, School & Hospital of Stomatology, Wuhan University, Wuhan 430072, China. ²Department of Oral & Maxillofacial Head Neck Oncology, School & Hospital of Stomatology, Wuhan University, Wuhan 430079, Hubei, China. ³Department of Prosthodontics, School and Hospital of Stomatology, Wuhan University, Wuhan, China. ⁴School of Dentistry, The University of Queensland, Brisbane, QLD 4066, Australia. ⁵Institute of Biomedical Health Technology and Engineering, Shenzhen Bay Laboratory, Shenzhen 518132, China.

Received: 6 December 2023 Accepted: 18 March 2024

Published online: 29 March 2024

References

- Xia C, Dong X, Li H, Cao M, Sun D, He S, et al. Cancer statistics in China and United States, 2022: profiles, trends, and determinants. *Chin Med J*. 2022;135(5):584–90.
- Gerashchenko TS, Schegoleva AA, Khozyainova AA, Choinzonov EL, Denisov EV. Metastasis prevention: how to catch metastatic seeds. *Biochim Biophys Acta Rev Cancer*. 2023;1878(3):188867.
- Steeg PS. Targeting metastasis. *Nat Rev Cancer*. 2016;16(4):201–18.
- Sun J, Wu S, Jin Z, Ren S, Cho WC, Zhu C, et al. Lymph node micro-metastasis in non-small cell lung cancer. *Biomed Pharmacother*. 2022;149:112817.
- Achen MG, Stacker SA. Molecular control of lymphatic metastasis. *Ann N Y Acad Sci*. 2008;1131:225–34.
- O'Melia MJ, Lund AW, Thomas SN. The biophysics of lymphatic transport: engineering tools and immunological consequences. *Iscience*. 2019;22:28–43.
- Siegel RL, Miller KD, Fuchs HE, Jemal A. Cancer statistics, 2022. *CA Cancer J Clin*. 2022;72(1):7–33.
- Zhao G, Sun J, Ba K, Zhang Y. Significance of PET-CT for detecting occult lymph node metastasis and affecting prognosis in early-stage tongue squamous cell carcinoma. *Front Oncol*. 2020;10:386.
- Haugen BR, Alexander EK, Bible KC, Doherty GM, Mandel SJ, Nikiforov YE, et al. 2015 American Thyroid Association management guidelines for adult patients with thyroid nodules and differentiated thyroid cancer: the American Thyroid Association guidelines task force on thyroid nodules and differentiated thyroid cancer. *Thyroid*. 2016;26(1):1–133.

10. Malkiewicz B, Kielb P, Kobylański M, Karwacki J, Poterek A, Krajewski W, et al. Sentinel lymph node techniques in urologic oncology: current knowledge and application. *Cancers*. 2023;15(9):2495.
11. Ichiki Y, Taguchi R, Yanagihara A, Umesaki T, Nitanda H, Sakaguchi H, et al. Prognostic significance of lymph node dissection for lung cancer surgery: a narrative review. *J Thorac Dis*. 2023;15(4):2253–60.
12. Lawenda BD, Mondry TE, Johnstone PA. Lymphedema: a primer on the identification and management of a chronic condition in oncologic treatment. *CA Cancer J Clin*. 2009;59(1):8–24.
13. Roukos DH. Current status and future perspectives in gastric cancer management. *Cancer Treat Rev*. 2000;26(4):243–55.
14. Watanabe S, Asamura H. Lymph node dissection for lung cancer: significance, strategy, and technique. *J Thorac Oncol*. 2009;4(5):652–7.
15. Leong SP, Zuber M, Ferris RL, Kitagawa Y, Cabanas R, Levenback C, et al. Impact of nodal status and tumor burden in sentinel lymph nodes on the clinical outcomes of cancer patients. *J Surg Oncol*. 2011;103(6):518–30.
16. Eisenmenger LB, Wiggins RH 3rd. Imaging of head and neck lymph nodes. *Radiol Clin North Am*. 2015;53(1):115–32.
17. Briguori C, Tavano D, Colombo A. Contrast agent-associated nephrotoxicity. *Prog Cardiovasc Dis*. 2003;45(6):493–503.
18. Pasquini L, Napolitano A, Visconti E, Longo D, Romano A, Tomà P, et al. Gadolinium-based contrast agent-related toxicities. *CNS Drugs*. 2018;32(3):229–40.
19. Garcia J, Liu SZ, Louie AY. Biological effects of MRI contrast agents: gadolinium retention, potential mechanisms and a role for phosphorus. *Philos Trans A Math Phys Eng Sci*. 2017;375(2107):20170180.
20. Su Y, Yu B, Wang S, Cong H, Shen Y. NIR-II bioimaging of small organic molecule. *Biomaterials*. 2021;271:120717.
21. Torchilin VP. Passive and active drug targeting: drug delivery to tumors as an example. *Handb Exp Pharmacol*. 2010;197:3–53.
22. Fournier L, de La Taille T, Chauvierre C. Microbubbles for human diagnosis and therapy. *Biomaterials*. 2023;294:122025.
23. Huang Q, Liu Q, Lin L, Li FJ, Han Y, Song ZG. Reduction of arsenic toxicity in two rice cultivar seedlings by different nanoparticles. *Ecotoxicol Environ Saf*. 2018;159:261–71.
24. Christensen-Jeffries K, Couture O, Dayton PA, Eldar YC, Hynynen K, Kiessling F, et al. Super-resolution ultrasound imaging. *Ultrasound Med Biol*. 2020;46(4):865–91.
25. Sahoo SK, Labhasetwar V. Nanotech approaches to drug delivery and imaging. *Drug Discov Today*. 2003;8(24):1112–20.
26. Zwicke GL, Mansoori GA, Jeffery CJ. Utilizing the folate receptor for active targeting of cancer nanotherapeutics. *Nano Rev*. 2012;3:18496.
27. Hoshyar N, Gray S, Han H, Bao G. The effect of nanoparticle size on in vivo pharmacokinetics and cellular interaction. *Nanomedicine*. 2016;11(6):673–92.
28. Gao X, Cui Y, Levenson RM, Chung LW, Nie S. In vivo cancer targeting and imaging with semiconductor quantum dots. *Nat Biotechnol*. 2004;22(8):969–76.
29. Proulx ST, Luciani P, Christiansen A, Karaman S, Blum KS, Rinderknecht M, et al. Use of a PEG-conjugated bright near-infrared dye for functional imaging of rerouting of tumor lymphatic drainage after sentinel lymph node metastasis. *Biomaterials*. 2013;34(21):5128–37.
30. Zbyszynski P, Toraason I, Repp L, Kwon GS. Probing the subcutaneous absorption of a PEGylated FUD peptide nanomedicine via in vivo fluorescence imaging. *Nano Converg*. 2019;6(1):22.
31. Gu L, Deng H, Bai Y, Gao J, Wang X, Yue T, et al. Sentinel lymph node mapping in patients with breast cancer using a photoacoustic/ultrasound dual-modality imaging system with carbon nanoparticles as the contrast agent: a pilot study. *Biomed Opt Express*. 2023;14(3):1003–14.
32. Goodspeed AW. Experiments on the roentgen X-rays. *Science*. 1896;3(59):236–7.
33. Dewis JW. Aids in the diagnosis of surgical conditions of the stomach with especial reference to the characteristic x-ray appearance of the syphilitic hour-glass in contrast to those of simple ulcer and cancer. *Can Med Assoc J*. 1915;5(12):1056–69.
34. Warren S, Meyer RW. Lymph node metastasis of sarcoma. *Am J Pathol*. 1938;14(5):605–620.1.
35. Ambrose J. CT scanning: a backward look. *Semin Roentgenol*. 1977;12(1):7–11.
36. Vigouroux RP, Baurand C, Gomez A, Legre J, Regis H, Debaene A. Value of computerized axial tomography in cranio-cerebral injuries. *Neurochirurgie*. 1976;22(3):281–91.
37. Mancuso AA, Hanafee WN, Juillard GJ, Winter J, Calcaterra TC. The role of computed tomography in the management of cancer of the larynx. *Radiology*. 1977;124(1):243–4.
38. Carter SK. Importance of controlling the regional draining lymph nodes in breast cancer. *Cancer Clin Trials*. 1978;1(3):227–33.
39. Polomska AK, Proulx ST. Imaging technology of the lymphatic system. *Adv Drug Deliv Rev*. 2021;170:294–311.
40. Husband JE, Robinson L, Thomas G. Contrast enhancing lymph nodes in bladder cancer: a potential pitfall on CT. *Clin Radiol*. 1992;45(6):395–8.
41. Nimura H, Narimiya N, Mitsumori N, Yamazaki Y, Yanaga K, Urashima M. Infrared ray electronic endoscopy combined with indocyanine green injection for detection of sentinel nodes of patients with gastric cancer. *Br J Surg*. 2004;91(5):575–9.
42. Helfand WH, Cowen DL. Evolution of pharmaceutical oral dosage forms. *Pharm Hist*. 1983;25(1):3–18.
43. Kreuter J, Speiser PP. In vitro studies of poly(methyl methacrylate) adjuvants. *J Pharm Sci*. 1976;65(11):1624–7.
44. Nefzger M, Kreuter J, Voges R, Liehl E, Czok R. Distribution and elimination of polymethyl methacrylate nanoparticles after peroral administration to rats. *J Pharm Sci*. 1984;73(9):1309–11.
45. Pouliquen D, Perdriset R, Ermias A, Akoka S, Jallet P, Le Jeune JJ. Superparamagnetic iron oxide nanoparticles as a liver MRI contrast agent: contribution of microencapsulation to improved biodistribution. *Magn Reson Imaging*. 1989;7(6):619–27.
46. Anzai Y, Blackwell KE, Hirschowitz SL, Rogers JW, Sato Y, Yuh WTC, et al. Initial clinical-experience with dextran-coated superparamagnetic iron-oxide for detection of lymph-node metastases in patients with head and neck-cancer. *Radiology*. 1994;192(3):709–15.
47. Kobayashi H, Kawamoto S, Sakai Y, Choyke PL, Star RA, Brechbiel MW, et al. Lymphatic drainage imaging of breast cancer in mice by micro-magnetic resonance lymphangiography using a nano-size paramagnetic contrast agent. *J Natl Cancer Inst*. 2004;96(9):703–8.
48. Song KH, Kim C, Cobley CM, Xia Y, Wang LV. Near-infrared gold nanocages as a new class of tracers for photoacoustic sentinel lymph node mapping on a rat model. *Nano Lett*. 2009;9(1):183–8.
49. Boll H, Nittka S, Doyon F, Neumaier M, Marx A, Kramer M, et al. Micro-CT based experimental liver imaging using a nanoparticulate contrast agent: a longitudinal study in mice. *PLoS ONE*. 2011;6(9): e25692.
50. Hur S, Kim J, Ratnam L, Itkin M. Lymphatic intervention, the frontline of modern lymphatic medicine: Part I. history, anatomy, physiology, and diagnostic imaging of the lymphatic system. *Korean J Radiol*. 2023;24(2):95–108.
51. Ohhashi T, Mizuno R, Ikomi F, Kawai Y. Current topics of physiology and pharmacology in the lymphatic system. *Pharmacol Ther*. 2005;105(2):165–88.
52. Ahuja A, Ying M. Grey-scale sonography in assessment of cervical lymphadenopathy: review of sonographic appearances and features that may help a beginner. *Br J Oral Maxillofac Surg*. 2000;38(5):451–9.
53. Vassallo P, Edel G, Roos N, Naguib A, Peters PE. In-vitro high-resolution ultrasonography of benign and malignant lymph nodes: a sonographic-pathologic correlation. *Invest Radiol*. 1993;28(8):698–705.
54. Ying M, Bhatia KS, Lee YP, Yuen HY, Ahuja AT. Review of ultrasonography of malignant neck nodes: greyscale, Doppler, contrast enhancement and elastography. *Cancer Imaging*. 2014;13(4):658–69.
55. Johnson JT. A surgeon looks at cervical lymph nodes. *Radiology*. 1990;175(3):607–10.
56. Vassallo P, Wernecke K, Roos N, Peters PE. Differentiation of benign from malignant superficial lymphadenopathy: the role of high-resolution US. *Radiology*. 1992;183(1):215–20.
57. Ahuja AT, Chow L, Chick W, King W, Metreweli C. Metastatic cervical nodes in papillary carcinoma of the thyroid: ultrasound and histological correlation. *Clin Radiol*. 1995;50(4):229–31.
58. Ying M, Ahuja AT, Evans R, King W, Metreweli C. Cervical lymphadenopathy: sonographic differentiation between tuberculous nodes and nodal metastases from non-head and neck carcinomas. *J Clin Ultrasound*. 1998;26(8):383–9.
59. Elsholtz FHJ, Asbach P, Haas M, Becker M, Beets-Tan RGH, Thoeny HC, et al. Introducing the node reporting and data system 1.0 (Node-RADS):

- a concept for standardized assessment of lymph nodes in cancer. *Eur Radiol.* 2021;31(8):6116–24.
60. Maggialelli N, Greco CN, Lucarelli NM, Morelli C, Cianci V, Sasso S, et al. Applications of new radiological scores: the Node-rads in colon cancer staging. *Radiol Med.* 2023;128(11):1287–95.
 61. Leonardo C, Flammia RS, Lucciola S, Proietti F, Pecoraro M, Bucca B, et al. Performance of node-RADS scoring system for a standardized assessment of regional lymph nodes in bladder cancer patients. *Cancers.* 2023;15(3):580.
 62. Loch FN, Beyer K, Kreis ME, Kamphues C, Rayya W, Schineis C, et al. Diagnostic performance of node reporting and data system (Node-RADS) for regional lymph node staging of gastric cancer by CT. *Eur Radiol.* 2023. <https://doi.org/10.1007/s00330-023-10352-5>.
 63. Meyer HJ, Schnarkowski B, Pappisch J, Kerckhoff T, Wirtz H, Höhn AK, et al. CT texture analysis and node-RADS CT score of mediastinal lymph nodes—diagnostic performance in lung cancer patients. *Cancer Imaging.* 2022;22(1):75.
 64. Schmidtschonbein GW. Microlymphatics and lymph-flow. *Physiol Rev.* 1990;70(4):987–1028.
 65. Niikura K, Matsunaga T, Suzuki T, Kobayashi S, Yamaguchi H, Orba Y, et al. Gold nanoparticles as a vaccine platform: influence of size and shape on immunological responses in vitro and in vivo. *ACS Nano.* 2013;7(5):3926–38.
 66. Li Z, Sun L, Zhang Y, Dove AP, O'Reilly RK, Chen G. Shape effect of glyconanoparticles on macrophage cellular uptake and immune response. *ACS Macro Lett.* 2016;5(9):1059–64.
 67. Xiao K, Li Y, Luo J, Lee JS, Xiao W, Gonik AM, et al. The effect of surface charge on in vivo biodistribution of PEG-oligocholic acid based micellar nanoparticles. *Biomaterials.* 2011;32(13):3435–46.
 68. Song C, Xu W, Wei Z, Ou C, Wu J, Tong J, et al. Anti-LDLR modified TPZ@Ce6-PEG complexes for tumor hypoxia-targeting chemo-/radio-/photodynamic/photothermal therapy. *J Mater Chem B.* 2020;8(4):648–54.
 69. Luo M, Samandi LZ, Wang Z, Chen ZJ, Gao J. Synthetic nanovaccines for immunotherapy. *J Control Release.* 2017;263:200–10.
 70. Lee S, Margolin K. Cytokines in cancer immunotherapy. *Cancers.* 2011;3(4):3856–93.
 71. Zhao J, Ren Y, Chen J, Zheng J, Sun D. Viral pathogenesis, recombinant vaccines, and oncolytic virotherapy: applications of the canine distemper virus reverse genetics system. *Viruses.* 2020;12(3):339.
 72. Gawali P, Saraswat A, Bhide S, Gupta S, Patel K. Human solid tumors and clinical relevance of the enhanced permeation and retention effect: a 'golden gate' for nanomedicine in preclinical studies? *Nanomedicine.* 2023;18(2):169–90.
 73. Swartz MA, Kaipainen A, Netti PA, Brekken C, Boucher Y, Grodzinsky AJ, et al. Mechanics of interstitial-lymphatic fluid transport: theoretical foundation and experimental validation. *J Biomech.* 1999;32(12):1297–307.
 74. Wilson DS, Hirosue S, Raczky MM, Bonilla-Ramirez L, Jeanbart L, Wang R, et al. Antigens reversibly conjugated to a polymeric glyco-adjuvant induce protective humoral and cellular immunity. *Nat Mater.* 2019;18(2):175–85.
 75. van Broekhoven CL, Parish CR, Demangel C, Britton WJ, Altin JG. Targeting dendritic cells with antigen-containing liposomes: a highly effective procedure for induction of antitumor immunity and for tumor immunotherapy. *Cancer Res.* 2004;64(12):4357–65.
 76. van Dinther D, Veninga H, Revet M, Hoogterp L, Olessek K, Grabowska J, et al. Comparison of protein and peptide targeting for the development of a CD169-based vaccination strategy against melanoma. *Front Immunol.* 2018;9:1997.
 77. Cai S, Alhowsyan AA, Yang Q, Forrest WC, Shnyder Y, Forrest ML. Cellular uptake and internalization of hyaluronan-based doxorubicin and cisplatin conjugates. *J Drug Target.* 2014;22(7):648–57.
 78. Zheutlin N, Shanbrom E. Contrast visualization of lymph nodes. *Radiology.* 1958;71(5):702–8.
 79. Chopra A. ZW800-1, a zwitterionic near-infrared fluorophore, and its cyclic RGD peptide derivative cyclo-(RGDyK)-ZW800-1. *Molecular Imaging and Contrast Agent Database (MICAD).* Bethesda (MD). 2004.
 80. Abdi EA, Terry T. Lymphography and computed tomography in lymph node metastases from malignant melanoma. *Acta Radiol.* 1988;29(4):391–4.
 81. Stark DD, Clark OH, Moss AA. Magnetic resonance imaging of the thyroid, thymus, and parathyroid glands. *Surgery.* 1984;96(6):1083–91.
 82. Dietrich CF, Liesen M, Buhl R, Herrmann G, Kirchner J, Caspary WF, et al. Detection of normal mediastinal lymph nodes by ultrasonography. *Acta Radiol.* 1997;38(6):965–9.
 83. Hallouard F, Anton N, Choquet P, Constantinesco A, Vandamme T. Iodinated blood pool contrast media for preclinical X-ray imaging applications—a review. *Biomaterials.* 2010;31(24):6249–68.
 84. Sugi K, Fukuda M, Nakamura H, Kaneda Y. Comparison of three tracers for detecting sentinel lymph nodes in patients with clinical N0 lung cancer. *Lung Cancer.* 2003;39(1):37–40.
 85. Engeset A. Lymphadenography after acute massive irradiation of the lymph nodes and after lymph nodal dissection (experimental study on rats). *Minerva Chir.* 1961;16:729–32.
 86. Ottaviani G. The lymph node and lymphnodography. *Arch Ital Chir.* 1961;87:601–12.
 87. Ege GN. Radiocolloid lymphoscintigraphy in neoplastic disease. *Cancer Res.* 1980;40(8 Pt 2):3065–71.
 88. Iimura T, Fukushima Y, Kumita S, Ogawa R, Hyakusoku H. Estimating lymphodynamic conditions and lymphovenous anastomosis efficacy using (99m)Tc-phytate lymphoscintigraphy with SPECT-CT in patients with lower-limb lymphedema. *Plast Reconstr Surg Glob Open.* 2015;3(5):e404.
 89. Olson JA Jr, Fey J, Winawer J, Borgen PI, Cody HS 3rd, Van Zee KJ, et al. Sentinel lymphadenectomy accurately predicts nodal status in T2 breast cancer. *J Am Coll Surg.* 2000;191(6):593–9.
 90. Dilege E, Celik B, Falay O, Boge M, Sucu S, Toprak S, et al. SPECT/CT lymphoscintigraphy accurately localizes clipped and sentinel nodes after neoadjuvant chemotherapy in node-positive breast cancer. *Clin Nucl Med.* 2023. <https://doi.org/10.1097/RLU.0000000000004669>.
 91. Vander Heiden MG, Cantley LC, Thompson CB. Understanding the Warburg effect: the metabolic requirements of cell proliferation. *Science.* 2009;324(5930):1029–33.
 92. Herbrink M, Treffert J, Geiger B, Riegger C, Hartung V, Rosenbaum-Krumme SJ, et al. Diagnostic accuracy of virtual 18F-FDG PET/CT bronchoscopy for the detection of lymph node metastases in non-small cell lung cancer patients. *J Nucl Med.* 2011;52(10):1520–5.
 93. Bille A, Pelosi E, Skanjeti A, Arena V, Errico L, Borasio P, et al. Preoperative intrathoracic lymph node staging in patients with non-small-cell lung cancer: accuracy of integrated positron emission tomography and computed tomography. *Eur J Cardiothorac Surg.* 2009;36(3):440–5.
 94. Munch S, Marr L, Feuerecker B, Dapper H, Braren R, Combs SE, et al. Impact of (18)F-FDG-PET/CT on the identification of regional lymph node metastases and delineation of the primary tumor in esophageal squamous cell carcinoma patients. *Strahlenther Onkol.* 2020;196(9):787–94.
 95. Yoon YC, Lee KS, Shim YM, Kim BT, Kim K, Kim TS. Metastasis to regional lymph nodes in patients with esophageal squamous cell carcinoma: CT versus FDG PET for presurgical detection prospective study. *Radiology.* 2003;227(3):764–70.
 96. Nakamura H, Miwa K, Haruki T, Adachi Y, Fujioka S, Taniguchi Y. Multifocal nodular lymphoid hyperplasia of the lung differently identified by 18F-fluorodeoxyglucose positron emission tomography (FDG-PET). *Thorac Cardiovasc Surg.* 2009;57(7):439–40.
 97. Suga K, Yasuhiko K, Hiyama A, Hori K, Tanaka N, Ueda K. F-18 FDG PET/CT findings in a case of multifocal nodular lymphoid hyperplasia of the lung. *Clin Nucl Med.* 2009;34(6):374–6.
 98. Manta R, Muteganya R, Beun AJ, Fallas J, Poppe KG. An exceptional cause of increased (18)F-fluorodeoxyglucose uptake on PET/CT in a thyroid nodule. *Diagnostics.* 2023;13(2):296.
 99. Pykett IL, Hinshaw WS, Buonanno FS, Brady TJ, Burt CT, Goldman MR, et al. Physical principles of NMR imaging. *Curr Probl Cancer.* 1982;7(3):37–50.
 100. Doyle FH, Gore JC, Pennock JM, Bydder GM, Orr JS, Steiner RE, et al. Imaging of the brain by nuclear magnetic resonance. *Lancet.* 1981;2(8237):53–7.
 101. Nelson KL, Runge VM. Basic principles of MR contrast. *Top Magn Reson Imaging.* 1995;7(3):124–36.
 102. Runge VM, Jacobson S, Wood ML, Kaufman D, Adelman LS. MR imaging of rat brain glioma: Gd-DTPA versus Gd-DOTA. *Radiology.* 1988;166(3):835–8.

103. Xu H, Liu J, Huang Y, Zhou P, Ren J. MRI-based radiomics as response predictor to radiochemotherapy for metastatic cervical lymph node in nasopharyngeal carcinoma. *Br J Radiol.* 2021;94(1122):20201212.
104. Rudnick MR, Wahba IM, Leonberg-Yoo AK, Miskulin D, Litt HI. Risks and options with gadolinium-based contrast agents in patients With CKD: a review. *Am J Kidney Dis.* 2021;77(4):517–28.
105. Semelka RC, Ramalho M, AlObaidy M, Ramalho J. Gadolinium in humans: a family of disorders. *AJR Am J Roentgenol.* 2016;207(2):229–33.
106. Semelka RC, Ramalho M. Gadolinium deposition disease: current state of knowledge and expert opinion. *Invest Radiol.* 2023;58(8):523–9. <https://doi.org/10.1097/RLI.0000000000000977>.
107. Cowling T, Frey N. CADTH Rapid Response Reports. Macrocyclic and linear gadolinium based contrast agents for adults undergoing magnetic resonance imaging: a review of safety. Ottawa (ON): Canadian Agency for Drugs and Technologies in Health Copyright © 2019 Canadian Agency for Drugs and Technologies in Health. 2019.
108. Shahid I, Joseph A, Lancelot E. Use of real-life safety data from international pharmacovigilance databases to assess the importance of symptoms associated with gadolinium exposure. *Invest Radiol.* 2022;57(10):664–73.
109. Frangioni JV. In vivo near-infrared fluorescence imaging. *Curr Opin Chem Biol.* 2003;7(5):626–34.
110. Vahrmeijer AL, Hutteman M, van der Vorst JR, van de Velde CJ, Frangioni JV. Image-guided cancer surgery using near-infrared fluorescence. *Nat Rev Clin Oncol.* 2013;10(9):507–18.
111. Noh YW, Park HS, Sung MH, Lim YT. Enhancement of the photostability and retention time of indocyanine green in sentinel lymph node mapping by anionic polyelectrolytes. *Biomaterials.* 2011;32(27):6551–7.
112. Hutteman M, Mieog JS, van der Vorst JR, Liefers GJ, Putter H, Löwik CW, et al. Randomized, double-blind comparison of indocyanine green with or without albumin premixing for near-infrared fluorescence imaging of sentinel lymph nodes in breast cancer patients. *Breast Cancer Res Treat.* 2011;127(1):163–70.
113. Hojo T, Nagao T, Kikuyama M, Akashi S, Kinoshita T. Evaluation of sentinel node biopsy by combined fluorescent and dye method and lymph flow for breast cancer. *Breast.* 2010;19(3):210–3.
114. Murawa D, Hirche C, Dresel S, Hünerbein M. Sentinel lymph node biopsy in breast cancer guided by indocyanine green fluorescence. *Br J Surg.* 2009;96(11):1289–94.
115. Kitai T, Inomoto T, Miwa M, Shikayama T. Fluorescence navigation with indocyanine green for detecting sentinel lymph nodes in breast cancer. *Breast Cancer.* 2005;12(3):211–5.
116. Hirche C, Murawa D, Mohr Z, Kneif S, Hünerbein M. ICG fluorescence-guided sentinel node biopsy for axillary nodal staging in breast cancer. *Breast Cancer Res Treat.* 2010;121(2):373–8.
117. Bergholt MS, Zheng W, Lin K, Ho KY, Teh M, Yeoh KG, et al. Combining near-infrared-excited autofluorescence and Raman spectroscopy improves in vivo diagnosis of gastric cancer. *Biosens Bioelectron.* 2011;26(10):4104–10.
118. Gashev AA, Nagai T, Bridenbaugh EA. Indocyanine green and lymphatic imaging: current problems. *Lymphat Res Biol.* 2010;8(2):127–30.
119. Li J, Jiang B, Lin C, Zhuang Z. Fluorescence tomographic imaging of sentinel lymph node using near-infrared emitting bioreducible dextran nanogels. *Int J Nanomed.* 2014;9:5667–82.
120. Park JH, Berth F, Wang C, Wang S, Choi JH, Park SH, et al. Mapping of the perigastric lymphatic network using indocyanine green fluorescence imaging and tissue marking dye in clinically advanced gastric cancer. *Eur J Surg Oncol.* 2022;48(2):411–7.
121. Welsher K, Sherlock SP, Dai H. Deep-tissue anatomical imaging of mice using carbon nanotube fluorophores in the second near-infrared window. *Proc Natl Acad Sci USA.* 2011;108(22):8943–8.
122. Narayanan R, Kenney MC, Kamjoo S, Trinh TH, Seigel GM, Resende GP, et al. Toxicity of indocyanine green (ICG) in combination with light on retinal pigment epithelial cells and neurosensory retinal cells. *Curr Eye Res.* 2005;30(6):471–8.
123. Chen Y, Zhu S, Chen H, Yao L, Zhou J, Xu Y, et al. Diagnostic value of color Doppler ultrasonography in subacute thyroiditis. *Scanning.* 2022;2022:7456622.
124. Feng Y, Dong F, Xia X, Hu CH, Fan Q, Hu Y, et al. An adaptive Fuzzy C-means method utilizing neighboring information for breast tumor segmentation in ultrasound images. *Med Phys.* 2017;44(7):3752–60.
125. Nakamura T, Harashima H. Dawn of lipid nanoparticles in lymph node targeting: potential in cancer immunotherapy. *Adv Drug Deliv Rev.* 2020;167:78–88.
126. Zhang Q, Xin M, Yang S, Wu Q, Xiang X, Wang T, et al. Silica nanocarrier-mediated intracellular delivery of rapamycin promotes autophagy-mediated M2 macrophage polarization to regulate bone regeneration. *Mater Today Bio.* 2023;20:100623.
127. Xu C, He S, Wei X, Huang J, Xu M, Pu K. Activatable sonooafterglow nanoprobes for T cell imaging. *Adv Mater.* 2023;35: e2211651.
128. Morris RT, Joyrich RN, Naumann RW, Shah NP, Maurer AH, Strauss HW, et al. Phase II study of treatment of advanced ovarian cancer with folate-receptor-targeted therapeutic (vintafolide) and companion SPECT-based imaging agent (99mTc-etarfolatide). *Ann Oncol.* 2014;25(4):852–8.
129. Kleinmanns K, Bischof K, Anandan S, Popa M, Aklsen LA, Fosse V, et al. CD24-targeted fluorescence imaging in patient-derived xenograft models of high-grade serous ovarian carcinoma. *EBioMedicine.* 2020;56:102782.
130. Fonnes T, Strand E, Fasmer KE, Berg HF, Espedal H, Sortland K, et al. Near-infrared fluorescent imaging for monitoring of treatment response in endometrial carcinoma patient-derived xenograft models. *Cancers.* 2020;12(2):370.
131. Espedal H, Berg HF, Fonnes T, Fasmer KE, Krakstad C, Haldorsen IS. Feasibility and utility of MRI and dynamic (18F)-FDG-PET in an orthotopic organoid-based patient-derived mouse model of endometrial cancer. *J Transl Med.* 2021;19(1):406.
132. Thakor AS, Jokerst JV, Ghanouni P, Campbell JL, Mittra E, Gambhir SS. Clinically approved nanoparticle imaging agents. *J Nucl Med.* 2016;57(12):1833–7.
133. Ong BY, Ranganath SH, Lee LY, Lu F, Lee HS, Sahinidis NV, et al. Paclitaxel delivery from PLGA foams for controlled release in post-surgical chemotherapy against glioblastoma multiforme. *Biomaterials.* 2009;30(18):3189–96.
134. Monterrubio C, Pascual-Pasto G, Cano F, Vila-Ubach M, Manzanares A, Schaiquevich P, et al. SN-38-loaded nanofiber matrices for local control of pediatric solid tumors after subtotal resection surgery. *Biomaterials.* 2016;79:69–78.
135. Bağó JR, Pegna GJ, Okolie O, Hingtgen SD. Fibrin matrices enhance the transplant and efficacy of cytotoxic stem cell therapy for post-surgical cancer. *Biomaterials.* 2016;84:42–53.
136. Bastiancich C, Danhier P, Pr at V, Danhier F. Anticancer drug-loaded hydrogels as drug delivery systems for the local treatment of glioblastoma. *J Control Release.* 2016;243:29–42.
137. Tamargo RJ, Myseros JS, Epstein JI, Yang MB, Chasin M, Brem H. Interstitial chemotherapy of the 9L gliosarcoma: controlled release polymers for drug delivery in the brain. *Cancer Res.* 1993;53(2):329–33.
138. Kang T, Zhu Q, Wei D, Feng J, Yao J, Jiang T, et al. Nanoparticles coated with neutrophil membranes can effectively treat cancer metastasis. *ACS Nano.* 2017;11(2):1397–411.
139. Wang H-E, Yu H-M, Lu Y-C, Heish N-N, Tseng Y-L, Huang K-L, et al. Internal radiotherapy and dosimetric study for ¹¹¹In/¹⁷⁷Lu-polyglylated liposomes conjugates in tumor-bearing mice. *Nucl Instrum Methods Phys Res Sect A.* 2006;569(2):533–7.
140. Sonvico F, Dubernet C, Colombo P, Couvreur P. Metallic colloid nanotechnology, applications in diagnosis and therapeutics. *Curr Pharm Des.* 2005;11(16):2095–105.
141. Yang R, Chen L, Wang Y, Zhang L, Zheng X, Yang Y, et al. Tumor microenvironment responsive metal nanoparticles in cancer immunotherapy. *Front Immunol.* 2023;14:1237361.
142. Farzin A, Etesami SA, Quint J, Memic A, Tamayol A. Magnetic nanoparticles in cancer therapy and diagnosis. *Adv Healthc Mater.* 2020;9(9): e1901058.
143. Shah S, Dhawan V, Holm R, Nagarsenker MS, Perrie Y. Liposomes: advancements and innovation in the manufacturing process. *Adv Drug Deliv Rev.* 2020;154–155:102–22.
144. Shariatnia Z, Jalali AM. Chitosan-based hydrogels: preparation, properties and applications. *Int J Biol Macromol.* 2018;115:194–220.

145. Jain KK. An overview of drug delivery systems. *Methods Mol Biol.* 2020;2059:1–54.
146. Oku N. Innovations in liposomal DDS technology and its application for the treatment of various diseases. *Biol Pharm Bull.* 2017;40(2):119–27.
147. Maurer AH, Elsinga P, Fanti S, Nguyen B, Oyen WJ, Weber WA. Imaging the folate receptor on cancer cells with ^{99m}Tc-etafolatide: properties, clinical use, and future potential of folate receptor imaging. *J Nucl Med.* 2014;55(5):701–4.
148. Banerjee S, Pillai MR, Ramamoorthy N. Evolution of Tc-99m in diagnostic radiopharmaceuticals. *Semin Nucl Med.* 2001;31(4):260–77.
149. Regnis JA, Robinson M, Bailey DL, Cook P, Hooper P, Chan HK, et al. Mucociliary clearance in patients with cystic fibrosis and in normal subjects. *Am J Respir Crit Care Med.* 1994;150(1):66–71.
150. Cintolesi V, Stanton AW, Bains SK, Cousins E, Peters AM, Purushotham AD, et al. Constitutively enhanced lymphatic pumping in the upper limbs of women who later develop breast cancer-related lymphedema. *Lymphat Res Biol.* 2016;14(2):50–61.
151. Alazraki NP, Eshima D, Eshima LA, Herda SC, Murray DR, Vansant JP, et al. Lymphoscintigraphy, the sentinel node concept, and the intraoperative gamma probe in melanoma, breast cancer, and other potential cancers. *Semin Nucl Med.* 1997;27(1):55–67.
152. Park HS, Nam SH, Kim J, Shin HS, Suh YD, Hong KS. Clear-cut observation of clearance of sustainable upconverting nanoparticles from lymphatic system of small living mice. *Sci Rep.* 2016;6:27407.
153. Niki Y, Ogawa M, Makiura R, Magata Y, Kojima C. Optimization of dendrimer structure for sentinel lymph node imaging: effects of generation and terminal group. *Nanomedicine.* 2015;11(8):2119–27.
154. Kim J, Archer PA, Thomas SN. Innovations in lymph node targeting nanocarriers. *Semin Immunol.* 2021;56:101534.
155. Cabral H, Makino J, Matsumoto Y, Mi P, Wu H, Nomoto T, et al. Systemic targeting of lymph node metastasis through the blood vascular system by using size-controlled nanocarriers. *ACS Nano.* 2015;9(5):4957–67.
156. Videira MA, Botelho MF, Santos AC, Gouveia LF, de Lima JJ, Almeida AJ. Lymphatic uptake of pulmonary delivered radiolabelled solid lipid nanoparticles. *J Drug Target.* 2002;10(8):607–13.
157. Rohner NA, Thomas SN. Melanoma growth effects on molecular clearance from tumors and biodistribution into systemic tissues versus draining lymph nodes. *J Control Release.* 2016;223:99–108.
158. Tseng YC, Xu Z, Guley K, Yuan H, Huang L. Lipid-calcium phosphate nanoparticles for delivery to the lymphatic system and SPECT/CT imaging of lymph node metastases. *Biomaterials.* 2014;35(16):4688–98.
159. Whitesides GM. The 'right' size in nanobiotechnology. *Nat Biotechnol.* 2003;21(10):1161–5.
160. Yetisgin AA, Cetinel S, Zuvim M, Kosar A, Kutlu O. Therapeutic nanoparticles and their targeted delivery applications. *Molecules.* 2020;25(9):2193.
161. Yudd AP, Kempf JS, Goydos JS, Stahl TJ, Feinstein RS. Use of sentinel node lymphoscintigraphy in malignant melanoma. *Radiographics.* 1999;19(2):343–53.
162. Mudun A, Murray DR, Herda SC, Eshima D, Shattuck LA, Vansant JP, et al. Early stage melanoma: lymphoscintigraphy, reproducibility of sentinel node detection, and effectiveness of the intraoperative gamma probe. *Radiology.* 1996;199(1):171–5.
163. Coxon AT, Desai R, Patel PR, Vellimana AK, Willie JT, Dowling JL, et al. A pilot study of lymphoscintigraphy with tracer injection into the human brain. *J Cereb Blood Flow Metab.* 2023. <https://doi.org/10.1177/0271678X231160891>.
164. Keskin DB, Anandappa AJ, Sun J, Tirosh I, Mathewson ND, Li S, et al. Neoantigen vaccine generates intratumoral T cell responses in phase Ib glioblastoma trial. *Nature.* 2019;565(7738):234–9.
165. Rosenberg SA, Yang JC, Restifo NP. Cancer immunotherapy: moving beyond current vaccines. *Nat Med.* 2004;10(9):909–15.
166. Mullard A. The cancer vaccine resurgence. *Nat Rev Drug Discov.* 2016;15(10):663–5.
167. Schilham MGM, Zamecnik P, Privé BM, Israël B, Rijkema M, Scheenen T, et al. Head-to-head comparison of (68)Ga-prostate-specific membrane antigen PET/CT and ferumoxtran-10-enhanced MRI for the diagnosis of lymph node metastases in prostate cancer patients. *J Nucl Med.* 2021;62(9):1258–63.
168. Mumprecht V, Honer M, Vigil B, Proulx ST, Trachsel E, Kaspar M, et al. In vivo imaging of inflammation- and tumor-induced lymph node lymphangiogenesis by immuno-positron emission tomography. *Cancer Res.* 2010;70(21):8842–51.
169. Sun Y, Xiao L, Wang Y, Liu C, Cao L, Zhai W, et al. Diagnostic value of dynamic (18)F-FDG PET/CT imaging in non-small cell lung cancer and FDG hypermetabolic lymph nodes. *Quant Imaging Med Surg.* 2023;13(4):2556–67.
170. AlRasheedi M, Han S, Thygesen H, Neilson M, Hendry F, Alkarn A, et al. A comparative evaluation of mediastinal nodal SUVmax and derived ratios from (18)F-FDG PET/CT to predict nodal metastases in non-small cell lung cancer. *Diagnostics.* 2023;13(7):120.
171. Rasouli Z, Riyahi-Alam N, Khoobi M, Haghgoo S, Gholibegloo E, Ebrahimpour A, et al. Lymph node metastases detection using Gd(2)O(3)@PCD as novel multifunctional contrast imaging agent in metabolic magnetic resonance molecular imaging. *Contrast Media Mol Imaging.* 2022;2022:5425851.
172. Lahaye MJ, Engelen SM, Kessels AG, de Bruine AP, von Meyenfeldt MF, van Engelshoven JM, et al. USPIO-enhanced MR imaging for nodal staging in patients with primary rectal cancer: predictive criteria. *Radiology.* 2008;246(3):804–11.
173. Xia M, Wu F, Yang Y, Lu W, Song M, Ma Z. The possibility of visualizing TGF-β1 expression in ApoE(-/-) mice atherosclerosis using MR targeted imaging. *Acta Radiol.* 2023. <https://doi.org/10.1177/0284185123115398>.
174. Fortuin A, van Asten J, Veltien A, Philips B, Hambroek T, Johst S, et al. Small suspicious lymph nodes detected on ultrahigh-field magnetic resonance imaging (MRI) in patients with prostate cancer with high risk of nodal metastases: the first in-patient study on ultrasmall superparamagnetic iron oxide-enhanced 7T MRI. *Eur Urol.* 2023;83(4):375–7.
175. Koh DM, George C, Temple L, Collins DJ, Toomey P, Raja A, et al. Diagnostic accuracy of nodal enhancement pattern of rectal cancer at MRI enhanced with ultrasmall superparamagnetic iron oxide: findings in pathologically matched mesorectal lymph nodes. *AJR Am J Roentgenol.* 2010;194(6):W505–13.
176. Driessen D, Zámečník P, Dijkema T, Pegge SAH, van Engen-van Grunsven ACH, Takes RP, et al. High-Accuracy nodal staging of head and neck cancer with USPIO-enhanced MRI: a new reading algorithm based on node-to-node matched histopathology. *Invest Radiol.* 2022;57(12):810–8.
177. Ma X, Wang S, Hu L, Feng S, Wu Z, Liu S, et al. Imaging characteristics of USPIO nanoparticles (< 5 nm) as MR contrast agent in vitro and in the liver of rats. *Contrast Media Mol Imaging.* 2019;2019:3687537.
178. Bourrinet P, Bengele HH, Bonnemain B, Dencausse A, Idee JM, Jacobs PM, et al. Preclinical safety and pharmacokinetic profile of ferumoxtran-10, an ultrasmall superparamagnetic iron oxide magnetic resonance contrast agent. *Invest Radiol.* 2006;41(3):313–24.
179. Islam T, Harisinghani MG. Overview of nanoparticle use in cancer imaging. *Cancer Biomark.* 2009;5(2):61–7.
180. Saxena V, Sadoqi M, Shao J. Indocyanine green-loaded biodegradable nanoparticles: preparation, physicochemical characterization and in vitro release. *Int J Pharm.* 2004;278(2):293–301.
181. Weiler M, Dixon JB. Differential transport function of lymphatic vessels in the rat tail model and the long-term effects of Indocyanine Green as assessed with near-infrared imaging. *Front Physiol.* 2013;4:215.
182. Hong G, Wu JZ, Robinson JT, Wang H, Zhang B, Dai H. Three-dimensional imaging of single nanotube molecule endocytosis on plasmonic substrates. *Nat Commun.* 2012;3:700.
183. Shou K, Qu C, Sun Y, Chen H, Chen S, Zhang L, et al. Multifunctional biomedical imaging in physiological and pathological conditions using a NIR-II probe. *Adv Funct Mater.* 2017;27(23):1700995.
184. Yang G, Mu X, Pan X, Tang Y, Yao Q, Wang Y, et al. Ligand engineering of Au(44) nanoclusters for NIR-II luminescent and photoacoustic imaging-guided cancer photothermal therapy. *Chem Sci.* 2023;14(16):4308–18.
185. Zhang XD, Chen J, Luo Z, Wu D, Shen X, Song SS, et al. Enhanced tumor accumulation of sub-2 nm gold nanoclusters for cancer radiation therapy. *Adv Healthc Mater.* 2014;3(1):133–41.
186. Dykman LA, Khlebtsov NG. Immunological properties of gold nanoparticles. *Chem Sci.* 2017;8(3):1719–35.
187. Skrabalak SE, Chen J, Au L, Lu X, Li X, Xia Y. Gold nanocages for biomedical applications. *Adv Mater.* 2007;19(20):3177–84.
188. Liu H, Hong G, Luo Z, Chen J, Chang J, Gong M, et al. Atomic-precision gold clusters for NIR-II imaging. *Adv Mater.* 2019;31(46): e1901015.

189. Verbeek FP, Troyan SL, Mieog JS, Liefers GJ, Moffitt LA, Rosenberg M, et al. Near-infrared fluorescence sentinel lymph node mapping in breast cancer: a multicenter experience. *Breast Cancer Res Treat.* 2014;143(2):333–42.
190. Tao Y, Zhang Y, Ju E, Ren H, Ren J. Gold nanocluster-based vaccines for dual-delivery of antigens and immunostimulatory oligonucleotides. *Nanoscale.* 2015;7(29):12419–26.
191. Song X, Zhu W, Ge X, Li R, Li S, Chen X, et al. A new class of NIR-II gold nanocluster-based protein biolabels for in vivo tumor-targeted imaging. *Angew Chem Int Ed Engl.* 2021;60(3):1306–12.
192. Gulla SK, Rao BR, Moku G, Jinka S, Nimmu NV, Khalid S, et al. In vivo targeting of DNA vaccines to dendritic cells using functionalized gold nanoparticles. *Biomater Sci.* 2019;7(3):773–88.
193. Chu B, Chen Z, Shi H, Wu X, Wang H, Dong F, et al. Fluorescence, ultrasonic and photoacoustic imaging for analysis and diagnosis of diseases. *Chem Commun.* 2023;59(17):2399–412.
194. Fu Q, Zhu R, Song J, Yang H, Chen X. Photoacoustic imaging: contrast agents and their biomedical applications. *Adv Mater.* 2019;31(6):e1805875.
195. Liu S, Wang H, Zhang C, Dong J, Liu S, Xu R, et al. In vivo photoacoustic sentinel lymph node imaging using clinically-approved carbon nanoparticles. *IEEE Trans Biomed Eng.* 2020;67(7):2033–42.
196. Pan D, Cai X, Yalaz C, Senpan A, Omanakuttan K, Wickline SA, et al. Photoacoustic sentinel lymph node imaging with self-assembled copper neodecanoate nanoparticles. *ACS Nano.* 2012;6(2):1260–7.
197. Fluorescence sensing. In: Lakowicz JR, editor. *Principles of fluorescence spectroscopy.* Boston: Springer US; 2006. p. 623–73.
198. Thompson WR, Brecht HF, Ivanov V, Yu AM, Dumani DS, Lawrence DJ, et al. Characterizing a photoacoustic and fluorescence imaging platform for preclinical murine longitudinal studies. *J Biomed Opt.* 2023;28(3):036001.
199. Xi L, Zhou G, Gao N, Yang L, Gonzalo DA, Hughes SJ, et al. Photoacoustic and fluorescence image-guided surgery using a multifunctional targeted nanoprobe. *Ann Surg Oncol.* 2014;21(5):1602–9.
200. Chen Z, Deán-Ben XL, Gottschalk S, Razansky D. Performance of photoacoustic and fluorescence imaging in detecting deep-seated fluorescent agents. *Biomed Opt Express.* 2018;9(5):2229–39.
201. Yang L, Mao H, Cao Z, Wang YA, Peng X, Wang X, et al. Molecular imaging of pancreatic cancer in an animal model using targeted multifunctional nanoparticles. *Gastroenterology.* 2009;136(5):1514–25.e2.
202. Lee JH, Huh YM, Jun YW, Seo JW, Jang JT, Song HT, et al. Artificially engineered magnetic nanoparticles for ultra-sensitive molecular imaging. *Nat Med.* 2007;13(1):95–9.
203. Lee SY, Jeon SJ, Jung S, Chung JJ, Ahn CH. Targeted multimodal imaging modalities. *Adv Drug Deliv Rev.* 2014;76:60–78.
204. Sinha R, Kim GJ, Nie S, Shin DM. Nanotechnology in cancer therapeutics: bioconjugated nanoparticles for drug delivery. *Mol Cancer Ther.* 2006;5(8):1909–17.
205. Barenholz Y. Doxil[®]—the first FDA-approved nano-drug: lessons learned. *J Control Release.* 2012;160(2):117–34.
206. Schön MP, Schön M. TLR7 and TLR8 as targets in cancer therapy. *Oncogene.* 2008;27(2):190–9.
207. Conniot J, Scomparin A, Peres C, Yeini E, Pozzi S, Matos AI, et al. Immunization with mannose-targeted nanovaccines and inhibition of the immune-suppressing microenvironment sensitizes melanoma to immune checkpoint modulators. *Nat Nanotechnol.* 2019;14(9):891–901.
208. Pan C, Wu J, Qing S, Zhang X, Zhang L, Yue H, et al. Biosynthesis of self-assembled proteinaceous nanoparticles for vaccination. *Adv Mater.* 2020;32(42):e2002940.
209. Zhu D, Hu C, Fan F, Qin Y, Huang C, Zhang Z, et al. Co-delivery of antigen and dual agonists by programmed mannose-targeted cationic lipid-hybrid polymersomes for enhanced vaccination. *Biomaterials.* 2019;206:25–40.
210. Dhodapkar MV, Sznol M, Zhao B, Wang D, Carvajal RD, Keohan ML, et al. Induction of antigen-specific immunity with a vaccine targeting NY-ESO-1 to the dendritic cell receptor DEC-205. *Sci Transl Med.* 2014;6(232):232ra51.
211. Chen Y, Wang B, Chen W, Wang T, Li M, Shen Z, et al. Co-delivery of dihydroartemisinin and indocyanine green by metal-organic framework-based vehicles for combination treatment of hepatic carcinoma. *Pharmaceutics.* 2022;14(10):2047.
212. Fu G, Liu W, Feng S, Yue X. Prussian blue nanoparticles operate as a new generation of photothermal ablation agents for cancer therapy. *Chem Commun.* 2012;48(94):11567–9.
213. Richter K, Haslbeck M, Buchner J. The heat shock response: life on the verge of death. *Mol Cell.* 2010;40(2):253–66.
214. Li J, Xie L, Li B, Yin C, Wang G, Sang W, et al. Engineering a hydrogen-sulfide-based nanomodulator to normalize hyperactive photothermal immunogenicity for combination cancer therapy. *Adv Mater.* 2021;33(22):e2008481.
215. Fix SM, Papadopoulou V, Velds H, Kasoji SK, Rivera JN, Borden MA, et al. Oxygen microbubbles improve radiotherapy tumor control in a rat fibrosarcoma model—a preliminary study. *PLoS ONE.* 2018;13(4):e0195667.
216. Huang SL, Hamilton AJ, Nagaraj A, Tiukinhoy SD, Klegerman ME, McPherson DD, et al. Improving ultrasound reflectivity and stability of echogenic liposomal dispersions for use as targeted ultrasound contrast agents. *J Pharm Sci.* 2001;90(12):1917–26.
217. Chen L, Zhou SF, Su L, Song J. Gas-mediated cancer bioimaging and therapy. *ACS Nano.* 2019;13(10):10887–917.
218. Wang Y, Zhang W, Sun P, Cai Y, Xu W, Fan Q, et al. A novel multimodal NIR-II nanoprobe for the detection of metastatic lymph nodes and targeting chemo-photothermal therapy in oral squamous cell carcinoma. *Theranostics.* 2019;9(2):391–404.
219. Pandit A, Zeugolis DL. Twenty-five years of nano-bio-materials: have we revolutionized healthcare? *Nanomedicine.* 2016;11(9):985–7.
220. Ventola CL. Progress in nanomedicine: approved and investigational nanodrugs. *Pharm Ther.* 2017;42(12):742–55.
221. Ernst LM, Mondragón L, Ramis J, Gustà MF, Yudina T, Casals E, et al. Exploring the long-term tissue accumulation and excretion of 3 nm cerium oxide nanoparticles after single dose administration. *Antioxidants.* 2023;12(3):765.
222. Carlander U, Moto TP, Desalegn AA, Yokel RA, Johanson G. Physiologically based pharmacokinetic modeling of nanoceria systemic distribution in rats suggests dose- and route-dependent biokinetics. *Int J Nanomed.* 2018;13:2631–46.
223. Kreyling WG, Holzwarth U, Hirn S, Schleh C, Wenk A, Schäffler M, et al. Quantitative biokinetics over a 28 day period of freshly generated, pristine, 20 nm silver nanoparticle aerosols in healthy adult rats after a single 1½-hour inhalation exposure. *Part Fibre Toxicol.* 2020;17(1):21.
224. Fratoddi I, Venditti I, Cametti C, Russo MV. How toxic are gold nanoparticles? The state-of-the-art. *Nano Res.* 2015;8(6):1771–99.
225. Sun C, Lee JS, Zhang M. Magnetic nanoparticles in MR imaging and drug delivery. *Adv Drug Deliv Rev.* 2008;60(11):1252–65.
226. Wang R, Song B, Wu J, Zhang Y, Chen A, Shao L. Potential adverse effects of nanoparticles on the reproductive system. *Int J Nanomed.* 2018;13:8487–506.
227. Rollerova E, Jurcovicova J, Mlynarcikova A, Sadlonova I, Bilanicova D, Wsolova L, et al. Delayed adverse effects of neonatal exposure to polymeric nanoparticle poly(ethylene glycol)-block-poly(lactide methyl ether) on hypothalamic-pituitary-ovarian axis development and function in Wistar rats. *Reprod Toxicol.* 2015;57:165–75.
228. Semmler-Behnke M, Lipka J, Wenk A, Hirn S, Schäffler M, Tian F, et al. Size dependent translocation and fetal accumulation of gold nanoparticles from maternal blood in the rat. *Part Fibre Toxicol.* 2014;11:33.
229. Ghalandari B, Asadollahi K, Ghorbani F, Ghalehbaghi S, Rafiee S, Komeili A, et al. Determinants of gold nanoparticle interactions with proteins: off-target effect study. *Spectrochim Acta A Mol Biomol Spectrosc.* 2022;269:120736.
230. Celá P, Veselá B, Matalová E, Večeřa Z, Buchtová M. Embryonic toxicity of nanoparticles. *Cells Tissues Organs.* 2014;199(1):1–23.
231. Cao W, Liu X, Huang X, Liu Z, Cao X, Gao W, et al. Hepatotoxicity-related oxidative modifications of thioredoxin 1/peroxiredoxin 1 induced by different cadmium-based quantum dots. *Anal Chem.* 2022;94(8):3608–16.
232. Jomova K, Baros S, Valko M. Redox active metal-induced oxidative stress in biological systems. *Transit Met Chem.* 2012;37(2):127–34.
233. Anselmo AC, Mitragotri S. Nanoparticles in the clinic: an update. *Bioeng Transl Med.* 2019;4(3):e10143.
234. Bu LL, Zhao ZL, Liu JF, Ma SR, Huang CF, Liu B, et al. STAT3 blockade enhances the efficacy of conventional chemotherapeutic

- agents by eradicating head neck stemloid cancer cell. *Oncotarget*. 2015;6(39):41944–58.
235. Bu LL, Yu GT, Deng WW, Mao L, Liu JF, Ma SR, et al. Targeting STAT3 signaling reduces immunosuppressive myeloid cells in head and neck squamous cell carcinoma. *Oncoimmunology*. 2016;5(5): e1130206.
 236. Sule N, Singh R, Srivastava DK. Alternative modes of binding of recombinant human histone deacetylase 8 to colloidal gold nanoparticles. *J Biomed Nanotechnol*. 2008;4(4):463–8.
 237. Ishii Y, Hattori Y, Yamada T, Uesato S, Maitani Y, Nagaoka Y. Histone deacetylase inhibitor prodrugs in nanoparticle vector enhanced gene expression in human cancer cells. *Eur J Med Chem*. 2009;44(11):4603–10.
 238. Kirchner C, Liedt T, Kudera S, Pellegrino T, Munoz Javier A, Gaub HE, et al. Cytotoxicity of colloidal CdSe and CdSe/ZnS nanoparticles. *Nano Lett*. 2005;5(2):331–8.
 239. Schöttler S, Becker G, Winzen S, Steinbach T, Mohr K, Landfester K, et al. Protein adsorption is required for stealth effect of poly(ethylene glycol)- and poly(phosphoester)-coated nanocarriers. *Nat Nanotechnol*. 2016;11(4):372–7.
 240. Simon J, Wolf T, Klein K, Landfester K, Wurm FR, Mailänder V. Hydrophilicity regulates the stealth properties of polyphosphoester-coated nanocarriers. *Angew Chem Int Ed Engl*. 2018;57(19):5548–53.
 241. Rabanel JM, Hildgen P, Banquy X. Assessment of PEG on polymeric particles surface, a key step in drug carrier translation. *J Control Release*. 2014;185:71–87.
 242. Rabanel JM, Faivre J, Tehrani SF, Laloz A, Hildgen P, Banquy X. Effect of the polymer architecture on the structural and biophysical properties of PEG-PLA nanoparticles. *ACS Appl Mater Interfaces*. 2015;7(19):10374–85.
 243. Bajaj AK, Gupta SC, Chatterjee AK, Singh KG. Contact sensitivity to polyethylene glycols. *Contact Dermatitis*. 1990;22(5):291–2.
 244. Cox F, Khalib K, Conlon N. PEG that reaction: a case series of allergy to polyethylene glycol. *J Clin Pharmacol*. 2021;61(6):832–5.
 245. Wenande E, Garvey LH. Immediate-type hypersensitivity to polyethylene glycols: a review. *Clin Exp Allergy*. 2016;46(7):907–22.
 246. Chen WA, Chang DY, Chen BM, Lin YC, Barenholz Y, Roffler SR. Antibodies against poly (ethylene glycol) activate innate immune cells and induce hypersensitivity reactions to PEGylated nanomedicines. *ACS Nano*. 2023;17(6):5757–72.
 247. Ishida T, Kiwada H. Accelerated blood clearance (ABC) phenomenon upon repeated injection of PEGylated liposomes. *Int J Pharm*. 2008;354(1–2):56–62.
 248. Elsadek NE, Hondo E, Shimizu T, Takata H, Abu Lila AS, Emam SE, et al. Impact of pre-existing or induced anti-PEG IgM on the pharmacokinetics of Peginterferon Alfa-2a (Pegasys) in mice. *Mol Pharm*. 2020;17(8):2964–70.
 249. Mima Y, Hashimoto Y, Shimizu T, Kiwada H, Ishida T. Anti-PEG IgM is a major contributor to the accelerated blood clearance of polyethylene glycol-conjugated protein. *Mol Pharm*. 2015;12(7):2429–35.
 250. Estapé Senti M, de Jongh CA, Dijkxhoorn K, Verhoef JF, Szebeni J, Storm G, et al. Anti-PEG antibodies compromise the integrity of PEGylated lipid-based nanoparticles via complement. *J Control Release*. 2022;341:475–86.
 251. Tenchov R, Sasso JM, Zhou QA. PEGylated lipid nanoparticle formulations: immunological safety and efficiency perspective. *Bioconjug Chem*. 2023;34(6):941–60.
 252. Wilhelm S, Tavares AJ, Dai Q, Ohta S, Audet J, Dvorak HF, et al. Analysis of nanoparticle delivery to tumours. *Nat Rev Mater*. 2016;1(5):1–2.
 253. Lahooti B, Akwii RG, Zahra FT, Sajib MS, Lamprou M, Alobaida A, et al. Targeting endothelial permeability in the EPR effect. *J Control Release*. 2023;361:212–35.
 254. Maeda H, Wu J, Sawa T, Matsumura Y, Hori K. Tumor vascular permeability and the EPR effect in macromolecular therapeutics: a review. *J Control Release*. 2000;65(1–2):271–84.
 255. Sun R, Xiang J, Zhou Q, Piao Y, Tang J, Shao S, et al. The tumor EPR effect for cancer drug delivery: current status, limitations, and alternatives. *Adv Drug Deliv Rev*. 2022;191:114614.
 256. Danhier F. To exploit the tumor microenvironment: since the EPR effect fails in the clinic, what is the future of nanomedicine? *J Control Release*. 2016;244(Pt A):108–21.
 257. LaVan DA, McGuire T, Langer R. Small-scale systems for in vivo drug delivery. *Nat Biotechnol*. 2003;21(10):1184–91.
 258. Surace C, Arpicco S, Dufaj-Wojcicki A, Marsaud V, Bouclier C, Clay D, et al. Lipoplexes targeting the CD44 hyaluronic acid receptor for efficient transfection of breast cancer cells. *Mol Pharm*. 2009;6(4):1062–73.
 259. Palomeras S, Ruiz-Martínez S, Puig T. Targeting breast cancer stem cells to overcome treatment resistance. *Molecules*. 2018;23(9):2193.
 260. Rezaei S, Kashanian S, Bahrami Y, Cruz LJ, Motiei M. Redox-sensitive and hyaluronic acid-functionalized nanoparticles for improving breast cancer treatment by cytoplasmic 17 α -methyltestosterone delivery. *Molecules*. 2020;25(5):1181.
 261. Akhoundova D, Rubin MA. Clinical application of advanced multi-omics tumor profiling: Shaping precision oncology of the future. *Cancer Cell*. 2022;40(9):920–38.
 262. Olivier M, Asmis R, Hawkins GA, Howard TD, Cox LA. The need for multi-omics biomarker signatures in precision medicine. *Int J Mol Sci*. 2019;20(19):4781.
 263. Xu Y, Su GH, Ma D, Xiao Y, Shao ZM, Jiang YZ. Technological advances in cancer immunity: from immunogenomics to single-cell analysis and artificial intelligence. *Signal Transduct Target Ther*. 2021;6(1):312.
 264. Luo J, Pan M, Mo K, Mao Y, Zou D. Emerging role of artificial intelligence in diagnosis, classification and clinical management of glioma. *Semin Cancer Biol*. 2023;91:110–23.
 265. Smolkova B, El Yamani N, Collins AR, Gutleb AC, Dusinska M. Nanoparticles in food: epigenetic changes induced by nanomaterials and possible impact on health. *Food Chem Toxicol*. 2015;77:64–73.
 266. Integrated Nanotechnology & Biomedical Sciences Laboratory. *Cancer Nanomedicine Repository*. <https://inbs.med.utoronto.ca/cnr/>. Accessed 20 Jan 2024.

Publisher's Note

Springer Nature remains neutral with regard to jurisdictional claims in published maps and institutional affiliations.